Polyolefin/Polyether Alternated Copolymers: Silyl-Modified Polymers as Promising Monocomponent Precursors to Adhesives

Supporting Information

Cyril Chauveau,[a,] Stéphane Fouquay,[b] Guillaume Michaud,[c] Frédéric Simon,[c] Jean-François Carpentier (ORCID: 0000-0002-9160-7662),[a,*] and Sophie M. Guillaume (ORCID: 0000-0003-2917-8657) [a,*]

[a] Univ Rennes, CNRS, ISCR (Institut des Sciences Chimiques de Rennes) – UMR 6226, F-35000 Rennes, France

[b] BOSTIK S.A., 420 rue d'Estienne d'Orves, 92705 Colombes Cedex, France

[c] BOSTIK, ZAC du Bois de Plaisance, 101, Rue du Champ Cailloux, F-60280 Venette, France

[*] Corresponding authors: jean-francois.carpentier@univ-rennes1; sophie.guillaume@univ-rennes1.fr

Content

Various approaches to the synthesis of PCOE/PPG$^{(*)}$ SMPs

- **CM of PPG$^{(*)}$: evaluation of various bis(trialkoxysilyl)alkene CTAs and of several catalysts.**
- **One-pot or two-pot, two-step ROMP/CM of COE catalyzed by G2 in the presence of CTA^{Et} and IM of PPG.**
- **One-pot, one-step ROIMP/CM of COE with PPG catalyzed by G2 in the presence of CTA^{Et}.**
- **One-pot, two-step ROIMP of COE and PPG catalyzed by G2 and CM in the presence of CTA^{Et} - Method II.**
- **One-pot, one-step ROIMP/CM of COE and PPG* catalyzed by G2 in the presence of CTA^{Et}: large-scale synthesis – Method I.**
- **Theoretical molar mass determination of α,ω-[Si(OEt)$_3$]$_2$-PCOE/PPG,PPG* SMPs prepared by ROMP/CM/IM**
- **Tensile testing of S1/G9 (1:1wt%)-cured SMPs.**

Scheme captions

Scheme S1. Illustration of the ROIMP synthesis of an alternated copolymer from a cycloolefin and a diacrylate, as first established by Grubbs and co-workers.[1]

Scheme S2. ALTMET synthesis of alternated copolymers.[2]

Scheme S3. Synthesis of PPG- and PPG*-based SMPs by CM of PPG and PPG*, respectively, using various catalysts in the presence of a trialkoxysilyl CTA.

Scheme S4. Synthesis of α,ω-[Si(OEt)$_3$]$_2$-PCOE/PPG by the sequential (one-pot or two-pot) two-step ROMP/CM of COE catalyzed by G2 in the presence of CTA^{Et} [3] and the subsequent IM of PPG.

Scheme S5. Synthesis of α,ω-[Si(OEt)$_3$]$_2$-PCOE/PPG by the one-pot, one-step ROIMP of COE with PPG / CM with CTA^{Et} catalyzed by G2 – Method I, as previously established with PPG*.[4]

Scheme S6. Formation of the four different chain-ends upon metathesis polymerization reactions (A: trialkoxysilyl, B: acrylate and vinyl, C: isomerized, chain-end groups) during the metathesis processes.

Scheme S7. Formation of ethylene during the ROIMP/CM process.[5]

Scheme S8. Illustration of the formation of polymer chains with a missing or an additional CH_2 during the CM of PCOE/PPG with the CTA (FG: trialkoxysilyl functional group).

Table captions

Table S1. Literature examples of ROIMP polymers, their A,B-alternations, molar mass values, and dispersities.1

Table S2. CM of PPG catalyzed by various ruthenium catalysts using several CTAs (Scheme S3).[a]

Table S3. CM of PPG* catalyzed by G2 using CTA2 (Scheme S3).[a]

Table S4. ROMP/CM of COE catalyzed by G2 in the presence of CTA^{Et} in CH_2Cl_2 at 40 °C during 24 h (Scheme S4).

Table S5. IM of PPG into α,ω-$[Si(Et)_3]_2$-PCOE prepolymer catalyzed by G2 in CH_2Cl_2 at 40 °C during 24 h (Scheme S4).

Table S6. One-pot, one-step ROIMP of COE with PPG and CM with CTA^{Et} catalyzed by G2 in CH_2Cl_2 at 40 °C during 24 h (Scheme S5).

Table S7. Large-scale ROIMP/CM of PCOE and PPG* catalyzed by G2 in the presence of CTA^{Et} (Scheme S5).[a]

Table S8. Thermal characteristics of α,ω-$[(EtO)_3Si]_2$-PCOE/PPG* SMPs prepared from the direct simpler tandem ROIMP/CM (one-pot, one-step) route – Method I (Table S7).[4]

Table S9. Rheological characteristics of the α,ω-$[(EtO)_3Si]_2$-PCOE/PPG* SMPs prepared from the direct simpler tandem ROIMP/CM (one-pot, one-step) route – Method I (Table S7).[4]

Table S10. Rheological data of α,ω-$[(EtO)_3Si]_2$-PCOE/PPG* SMPs synthesized by the one-pot, two-step ROIMP/CM route – large-scale synthesis (Method II) (Table S7).

Table S11. T_g and E' values measured by DMA analysis of S1/GF9(1:1wt%)-cured α,ω-$[(EtO)_3Si]_2$-PCOE/PPG* SMPs prepared in the present work from the tandem ROIMP/CM (one-pot, two-step) route – large-scale synthesis Method II (Table S7).

Figures captions

Figure S1. ^1H NMR spectrum (400 MHz, $CDCl_3$, 293 K**)** of PPG.

Figure S2. ^1H NMR spectrum (400 MHz, $CDCl_3$, 293 K**)** of PPG*.

Figure S3. ^{1}H and J-MOD (400 and 100 MHz, $CDCl_3$, 293 K) NMR spectra of Polyvest E100.

Figure S4. ^{1}H and J-MOD NMR spectra (400 and 100 MHz, 298 K, $CDCl_3$) of PPG-$CTA2_2$ isolated from the CM of PPG catalyzed by G2 using CTA2 (Table S2, entry 2); *: residual PPG-acrylate.

Figure S5. COSY NMR spectrum (400 MHz, $CDCl_3$, 293 K**)** of PPG-$CTA2_2$ isolated from the CM of PPG catalyzed by G2 using CTA2 (Table S2, entry 2).

Figure S6. HSQC NMR spectrum (100 & 400 MHz, $CDCl_3$, 293 K**)** of PPG-$CTA2_2$ isolated from the CM of PPG catalyzed by G2 using CTA2 (Table S2, entry 2).

Figure S7. FT-IR spectrum of PPG-$CTA2_2$ isolated from the CM of PPG catalyzed by G2 using CTA2 (Table S2, entry 2).

Figure S8. ^{1}H and J-MOD NMR spectra (400 and 100 MHz, 298 K, $CDCl_3$) of PPG*-$CTA2_2$ isolated from the CM of PPG* catalyzed by G2 using CTA2 (Table S3, entry 1); residual traces of *CTA2, and °CTA3-resulting from the self-metathesis of CTA2, not completely removed under vacuum presumably as the result of the high viscosity of the recovered polymer.

Figure S9. COSY NMR spectrum (400 MHz, $CDCl_3$, 293 K**)** of PPG*-$CTA2_2$ isolated from the CM of PPG* catalyzed by G2 using CTA2 (Table S3, entry 1).

Figure S10. HSQC NMR spectrum (100 & 400 MHz, $CDCl_3$, 293 K**)** of PPG*-$CTA2_2$ isolated from the CM of PPG* catalyzed by G2 using CTA2 (Table S3, entry 1).

Figure S11. HMBC NMR spectrum (100 & 400 MHz, $CDCl_3$, 293 K**)** of PPG*-$CTA2_2$ isolated from the CM of PPG* catalyzed by G2 using CTA2 (Table S3, entry 1).

Figure S12. FT-IR spectrum of PPG*-$CTA2_2$ isolated from the CM of PPG* catalyzed by G2 using CTA2 (Table S3, entry 1).

Figure S13. ESI-MS spectrum (DCTB matrix, NaI ionizing salt) of PPG*-$CTA2_2$ isolated from the CM of PPG* catalyzed by G2 using CTA2 (Table S3, entry 1); top and middle (zoomed) region: experimental spectrum, m/z = 900−5000 and m/z = 2684−2698, respectively; bottom : simulation for m/z = 2684−2698.

Figure S14. ^{1}H NMR spectrum (400 MHz, 23 °C, $CDCl_3$) of an α,ω-$[SiOEt_3)_2]$-PCOE/PPG crude-product prepared from the one-pot two-step ROMP/CM-IM of COE with PPG and CTA^{Et} catalyzed by G2 (Table S6 entry 2); *: unreacted CTA^{Et}.

Figure S15. ^{1}H and J-MOD NMR spectra (400 and 100 MHz, 23 °C, $CDCl_3$) of a PCOE/PPG sample isolated from the ROIMP of COE and PPG catalyzed by G2 (Table 1, entry 2).

Figure S16. COSY NMR spectrum (400 MHz, 23 °C, $CDCl_3$) of a PCOE/PPG sample isolated from the ROIMP of COE and PPG catalyzed by G2 (Table 1, entry 2).

Figure S17. HSQC NMR spectrum (100 and 400 MHz, 23 °C, $CDCl_3$) of a PCOE/PPG sample isolated from the ROIMP of COE and PPG catalyzed by G2 (Table 1, entry 2).

Figure S18. HMBC NMR spectrum (400 MHz, 23 °C, $CDCl_3$) of a PCOE/PPG sample isolated from the ROIMP of COE and PPG catalyzed by G2 (Table 1, entry 2).

Figure S19. Top: ESI-MS mass spectrum (NaI ionizing salt) of a PCOE/PPG sample isolated from the ROIMP of COE and PPG catalyzed by G2 and recovered after removal of the solvent under vacuum (Table 1, entry 2); bottom left: simulation and experimental spectra of a linear nonfunctional (or linear isomerized) PCOE (A)/PPG (B); bottom right: simulation and experimental spectra of a cyclic PCOE (A)/PPG (B).

Figure S20. COSY NMR spectrum (400 MHz, 23 °C, $CDCl_3$) of an α,ω-$[Si(OEt)_3]_2$-PCOE/PPG sample isolated from the one-pot, two-step ROIMP/CM of COE and PPG catalyzed by G2 in the presence of CTA^{Et} (Table 2, entry 6).

Figure S21. HSQC NMR spectrum (100 and 400 MHz, 23 °C, $CDCl_3$) of an α,ω-$[Si(OEt)_3]_2$-PCOE/PPG sample isolated from the one-pot, two-step ROIMP/CM of COE and PPG catalyzed by G2 in the presence of CTA^{Et} (Table 2, entry 6).

Figure S22. HMBC NMR spectrum (100 and 400 MHz, 23 °C, $CDCl_3$) of an α,ω-$[Si(OEt)_3]_2$-PCOE/PPG sample isolated from the one-pot, two-step ROIMP/CM of COE and PPG catalyzed by G2 in the presence of CTA^{Et} (Table 2, entry 6).

Figure S23. FT-IR spectrum of an α,ω-$[Si(OEt)_3]_2$-PCOE/PPG sample isolated from the one-pot, two-step ROIMP/CM of COE and PPG catalyzed by G2 in the presence of CTA^{Et} (Table 2, entry 6).

Figure S24. Top: ESI-MS mass spectrum (NaI ionizing salt; note that the Na is not made explicit in the formula of the polymer referred to as $A_pB_mCH_2FG$ and $A_pB_mFG_2$) of a α,ω-$[Si(OEt)_3]_2$-PCOE/PPG sample isolated from the one-pot, two-step ROIMP/CM of COE and PPG catalyzed by G2 in the presence of CTA^{Et} (Table 2, entry 6); bottom left: simulation and experimental spectra of a $Si(OEt)_3$-monofunctional PCOE/PPG; bottom right: simulation and experimental spectra of a $Si(OEt)_3]_2$-difunctional PCOE/PPG.

Figure S25. SEC traces (THF, 30 °C) of samples isolated from the two-step (blue – large-scale synthesis Method II) or one-step (red – Method I) ROIMP/CM of COE and PPG* catalyzed with G2 in the presence of CTA^{Et} ($[COE]_0/[PPG*]_0/[CTA^{Et}]_0$ = 1940:60:100; Table S7, entry 3, in blue, and entry 4, in red).

Figure S26. TGA (top-left: before curing; top-right: after curing) and DSC (bottom-left: first cooling step; bottom-right: first heating step)[6] thermograms of α,ω-[$(EtO)_3Si]_2$-PCOE/PPG* synthesized by the two-step ROIMP/CM route – large-scale synthesis Method II (Table 3).

Figure S27. DSC (under helium, 10 °C.min^{-1}) thermograms of PCOE^{20}/PPG2^{65}- CTA^{Et15}, first cooling step (blue) and second cooling step (orange).

Figure S28. Structure of Neostan S1 (Kaneka) and Geniosil GF9 (Wacker).

Figure S29. Illustration of the preparation of films derived from cured α,ω-[$(EtO)_3Si]_2$-PCOE/PPG* synthesized from the two-step ROIMP/CM Method II. From left to right: mixing of the SMP and the catalytic system (S1 (1wt%) and GF9 (1wt%)); formation of the film; the film after curing (Refer to the Experiential Section).

Figure S30. Examples of films obtained after curing of α,ω-[$(EtO)_3Si]_2$-PCOE/PPG* copolymers synthesized from the two-step ROIMP/CM Method II, with S1 (1wt%) and GF9 (1wt%).

Figure S31. Left: a film obtained after curing of α,ω-[$(EtO)_3Si]_2$-PCOE/PPG* copolymers synthesized from the two-step ROIMP/CM Method II, with S1 (1wt%) and GF9 (1wt%), on the press before cutting. Right: a tensile piece cut out this film.

Various approaches for the synthesis of PCOE/PPG$^{(*)}$ SMPs

CM of PPG$^{(*)}$: evaluation of various bis(trialkoxysilyl)alkene CTAs and of several catalysts. The preliminary experiments towards the synthesis of polyether-based SMPs were performed by the CM of PPG or PPG* with alkoxysilyl CTAs (Scheme S3). These aimed at evaluating the catalytic system upon screening a series of symmetrical trialkoxysilyl CTAs previously successfully used for the preparation of polyolefin-based SMPs,[3,4,7,8] and of several well-known ruthenium metathesis-effective catalysts (Tables S2,S3). This direct procedure enabled the successful preparation of the corresponding α,ω-bis(trialkoxysilyl) telechelic polyethers as evidenced by detailed NMR, FTIR and ESI-MS analyses, as described thereafter (Figures S4−S13).

The CM synthesis of SMPs based on PPG diacrylate (the one prepolymer providing simpler-to-analyze ^{1}H NMR spectra) was first explored upon screening five alkoxysilyl CTAs (CTA1−CTA4, CTA^{Et}) using G2 as a metathesis catalyst (Scheme S3), under typical operating conditions (CH_2Cl_2, 40 °C, 24 h, under a slight flow of argon to remove the ethylene formed during the reaction)[3,7-9] (Table S2, entries 1–5). The conversion of acrylate functions was monitored by ^{1}H NMR, upon comparing the characteristic PPG initial methylene signal at $\delta_{CH2=CH-}$ 6.5 ppm (Figure S1) with the distinctive signal of the corresponding α-unsaturated methine ester following the CM at $\delta_{CH2=CH-C(O)O}$ 7.0 ppm (Figure S4).

Both CTA^{Et} and CTA4 did not show any activity under the experimental conditions implemented (Table S2, entries 4–5). The lack of efficiency of CTA4 is reminiscent of its previous failed metathesis reactions, [3] and most likely resulted from the bulkiness of the C=C bond which impedes the approach of the metathesis catalyst. On the contrary, CTA^{Et} is usually highly effective in metathesis reactions (typically ROMP, ROMP/CM, CM).[3,7-8] Unsurprisingly, CTA1−3 were all found to be reactive in the CM reaction, as previously observed.[9] While CTA1 showed a poor efficiency (23% of acrylate conversion; the polymer could not be isolated from any purification attempts), both CTA2,3 displayed a high efficacy (98% and 92% of acrylate conversion, respectively; Table S2, entries 2,3). The structure of the SMP resulting from either CTA2 or CTA3 being the same, the use of CTA2 was next favored in light of its better reactivity in CM and its cheap commercial availability.

PPG-CTA2_2 was thus isolated as a brownish liquid from the CM reaction of PPG catalyzed by G2 using CTA2, after distillation under vacuum from the unreacted CTA2 (Table S2, entry 2). Signals from ^{1}H and J-MOD NMR spectra of the resulting polymer were assigned based on previous work, [9] and also on 2D NMR experiments (COSY, HSQC; Figures S5,S6). In particular, the observation of the resonances of the acrylate double bond methine hydrogens $H^{c,d}$ and carbon atoms $C^{c,d}$ hinted for a successful CM, while the FT-IR (Figure S7) analysis further confirmed the formation of the expected bis(trimethoxysilyl) end-capped polyether.

Several metathesis catalysts were next evaluated to optimize the productivity in the CM of PPG with CTA2 (Scheme S3; Table S2, entries 2, 6−15). The sequential addition of the ruthenium catalyst in three fractions over 2 h allowed to reach loadings of $[PPG]_0/[CTA2]_0/[Cat.]_0$ as high as 3000:7000:1, while an excess of CTA2 was used to enhance the conversion in acrylate (the excess of PPG acrylate was removed at the end of the reaction by distillation under vacuum). Grubbs 3rd generation catalyst (G3), Zhan 1B catalyst (Zhan) and Umicore M73 catalyst (M73) showed the lowest productivities (30–46% in acrylate conversion; Table S2, entries 10–15). While a good conversion was obtained with G2 (ca. 74% in acrylate conversion; Table S2, entries 6,7), the best productivity (turn over number (TON) = ca. 1500 $mol_{PPG}.mol_{cat}^{-1}.h^{-1}$, ca. 3150 $mol_{CTA2}.mol_{cat}^{-1}.h^{-1}$) was reached with Hoveyda-Grubbs 2nd generation catalyst (HG2) with ca. 90% in acrylate conversion

(Table S2, entries 8,9). Catalyst G2 affording the best compromise in terms of efficiency and competitive price, it was then favored in the following experiments.

Following the same strategy, the CM of the diacrylate end-capped poly(propyleneglycol$_{31}$diurethane) (PPG*) using CTA2 in the presence of G2 was then performed in CH_2Cl_2 at 40 °C under a flow of argon during 24 h (Scheme S3), affording 96% conversion in acrylate (Table S3, entry 1). ^{1}H, J-MOD, COSY, HSQC and HMBC NMR spectra of the isolated polymer (following removal of volatiles and drying under vacuum), along with the FT-IR spectrum and ESI-MS analysis, all supported the formation of the expected PPG* end-capped by trimethoxysilyl functions (Figures S8−S13). The SEC analysis of the recovered PPG*-CTA2$_2$ sample revealed three peaks ($M_{n,SEC}$ = 4000 (58%), 8000 (26%), 14000 g.mol^{-1} (12%); $Đ_M$ = 1.0 for each of them) slightly shifted to a higher molar mass value as compared to PPG* ($M_{n,SEC}$ = 3500 (59%), 7200 (24%), 12000 g.mol^{-1} (13%); $Đ_M$ =1.0 for each of them), corresponding to three distinct values of repeating units within PPG*, namely n = 1, 2 and 3, respectively, thus suggesting that the CM did not impact the polymer backbone, yet only proportionally increasing the molar mass according to the addition of the chain-end groups.

Larger amounts of PPG*-SMPs (ca. 100 g) were next prepared in order to evaluate the material and adhesive properties. Correspondingly, so as to compensate the reduction of the G2 catalyst activity observed when increasing ten times the prepolymer loading, the initial catalyst filling was raised up to [PPG*]$_0$/[CTA2]$_0$/[G2]$_0$ = 133:280:1, while G2 was sequentially added in five fractions over 2 h so as to avoid its potential degradation over time (Scheme S3; Table S3, entry 1 vs entries 2–5). The four batches of the thus prepared PPG*-CTA2$_2$ (Table S3, entries 2–5) were then mixed together and placed under vacuum at 70 °C during 2 h to remove the residual solvent and end-capping CTA2 components (Table S3, entry 6). Following this last purification step, the conversion in acrylate (97%; Table S3, entry

6) was found to be higher than the calculated average conversion determined from Table S3, entries 2–5 (ca. 90%). This difference is most likely arising from the persistent activity of the remaining G2 during the heating, which then drives the equilibrium toward the formation of the desired SMP upon removal of the ethylene under vacuum.

Although easy, straightforward and effective, the above mentioned CM of PPG* with the trimethoxysilyl CTA2 required a rather high catalyst loading (0.1 mol%) in comparison to optimized typical ROMP/CM processes (0.001 mol%).[3] Besides, the scale-up of the reaction required even higher loadings (0.2 mol%) which is a drawback. Another limitation of this post-polymerization method is that it does not enable to synthesize polymers of various structures due to the limitation from the chemical structure of the diacrylate prepolymers. Other more performant metathesis approaches were then sought (refer to the main manuscript Section *Synthesis and characterization of PCOE/PPG$^{(*)}$-based SMPs by a ROIMP/CM approach – Methods I and II, and other metathesis experiments described just below*).

One-pot or two-pot, two-step ROMP/CM of COE catalyzed by G2 in the presence of CTA^{Et} and IM of PPG. PCOE/PPG-based SMPs were prepared stepwise from the already reported α,ω-bis(triethoxysilyl) PCOE (α,ω-$[Si(OEt)_3]_2$-PCOE),[3] upon the subsequent IM of PPG moieties (Scheme S4). The PCOE SMP was first synthesized as previously reported from the ROMP of COE catalyzed by G2 using CTA^{Et} (Table S4), [3,4,7-10] and then either isolated following solvent removal under vacuum),[4] or used *in situ*, prior to the IM of PPG (Tables S4,S5), as described thereafter.

Typically, all polymerizations were performed according to the following procedure (Scheme S4, Table S4, entry 2). Under argon atmosphere, a Schlenk flask equipped with a magnetic stir bar, was charged sequentially with dry CH_2Cl_2 (5.0 mL), COE (1.29 g, 12 mmol) and CTA^{Et} (350 mg, 0.60 mmol). The resulting solution was heated at 40 °C and the polymerization was started upon addition, *via* a cannula, of a freshly prepared CH_2Cl_2 solution (1.0 mL) of G2 (5.0 mg, 5.9 μmol). The reaction mixture turned highly viscous within 2 min. The viscosity then slowly decreased over the following 10 min. After the desired reaction time (typically 24 h; reaction time was not necessarily optimized), CH_2Cl_2 (12.0 mL) and PPG (1.16 g, 3.9 mmol) (Scheme S4, Table S5, entry 2) were added and a freshly prepared CH_2Cl_2 solution (1.0 mL) of G2 (5.0 mg, 5.9 μmol) was charged *via* a cannula. After the desired reaction time (typically 24 h; reaction time was not necessarily optimized), volatiles (solvent and ethylene) were removed under vacuum. The copolymer was recovered without further purification, as a brownish viscous liquid at 25 °C, which is readily soluble in $CHCl_3$ and THF.

A conversion in acrylate of 50% and the release of 45% of ethylene − which attested the effective CM between the acrylate and the ring opened COE units (Scheme S7)[5] − were observed by ^{1}H NMR analyses from *in situ* experiments for $[G2]_0$ = 11 equiv. (Table S5, entry 2). Isolation of the α,ω-$[Si(OEt)_3]_2$-PCOE prepolymer prior to the IM enabled to improve these latter two values to 78 and 77%, respectively (Table S5, entry 3). Surprisingly, the introduction into the reaction medium of the catalyst in several fractions did not increase the conversion in acrylate nor the release of ethylene, but rather promoted the isomerization (vinyl/isom = 1.11 vs 0.07 and 0.5, Table S5, entries 3 vs 4,5, respectively). Both the molar mass values calculated ($M_{n,theo}$) and measured experimentally by SEC ($M_{n,SEC}$) systematically decreased following the PPG insertion step, most likely due to the high amount of vinyl and isomerized chain-ends formed.[3,4,7-9] Both $M_{n,theo}$ and $M_{n,SEC}$ values also varied proportionally to the conversion in acrylate and to the amount of ethylene released.

Although successful for the preparation of PCOE/PPG-based SMPs, this method requires the prior isolation of the PCOE prepolymer for a good reactivity of acrylate groups to be ultimately reached (58−78%), while the high amount of catalyst required remains another limitation (ca. 0.8 mol%, Table S5, entries 3–5). Another more efficient approach was thus desirable.

One-pot, one-step ROIMP/CM of COE with PPG catalyzed by G2 in the presence of CTA^{Et}. The one-pot, one-step ROIMP/CM of COE and PPG catalyzed by G2 in the presence of CTA^{Et} ($[COE]_0/[PPG]_0/[CTA^{Et}]_0/[G2]_0$ = 1500:500:100:2−10) was performed as previously reported for PPG* in CH_2Cl_2 at 40 °C during 24 h (Scheme S5; Table S6).[4] Note that this approach is the same as the one we previously reported,[4] yet it is in the present work performed in a <u>*diluted reaction medium*</u> ($[COE]_0 + [PPG]_0$ = 0.5 M vs $[COE]_0 + [PPG^*]_0$ = 6 M).

Typically, all polymerizations were performed according to the following procedure (Scheme S5) (Table S6, entry 3). Under an argon atmosphere, a Schlenk flask equipped with a magnetic stir bar was charged sequentially with CH_2Cl_2 (16.0 mL), COE (0.75 g, 6.8 mmol), PPG (0.68 g, 2.3 mmol) and CTA^{Et} (262 mg, 0.45 mmol). The resulting solution was heated at 40 °C and the polymerization was started upon addition, via a cannula, of a dry, freshly prepared CH_2Cl_2 solution (2.0 mL) of G2 (8.0 mg, 9.0 µmmol). The reaction mixture turned highly viscous within 2 min and the viscosity decreased over the following 10 min. The copolymer was recovered without further purification, as a brownish viscous liquid at 25 °C, which is readily soluble in $CHCl_3$ and THF. After the desired reaction time (typically 24 h; reaction time was not necessarily optimized), volatiles (solvent and ethylene) were removed under vacuum.

^1H NMR monitoring of the reaction showed a high conversion in CTA^{Et} (75−94%) even at the lowest loading in catalyst, whereas the conversion in acrylate remained mediocre reaching at best 52% with 10 equivalents of G2 added as a single aliquot (Table S6, entry 2). In all experiments, a high and rather constant amount of acrylate chain-ends was observed

(53−65%), regardless of the catalyst feed. When all the catalyst was added at once, the relative amounts of vinyl and isomerized chain-ends remained constant, whereas addition in two fractions again promoted the isomerization process (vinyl/isom = 0.04 vs. 0.94−1.06, Table S6, entries 1 vs 2,3). Noteworthy, the ratio between the various acrylate, vinyl, isomerized chain-ends depended both on the conversion in CTA^{Et} and in acrylate, and on the amount of ethylene released (Scheme S7); the more ethylene eliminated, the lower the respective content in vinyl and isomerized chain-ends in the recovered polymer. Also, a high amount of catalyst was required (ca. 10 equiv., 0.7 mol%) to improve the release of ethylene (26−44% vs 5%, Table S6, entries 1,2 vs 3). SEC analyses of the copolymers evidenced, besides a small trace around 150 $g.mol^{-1}$ corresponding to unreacted PPG, relatively low molar mass values (1500−2400 $g.mol^{-1}$) roughly consistent with the theoretical data (Table S6). NMR spectra of the recovered copolymers were in agreement with those reported for the alike α,ω-$[Si(OEt)_3]_2$-PCOE/PPG samples obtained from the above-mentioned previous ROMP/CM-IM method (Figure S14).

In light of the low conversion in PPG – even at high loadings of catalyst –, and given the impossibility to separate unreacted PPG from the final mixture, this tandem ROIMP/CM of COE and PPG in the presence of CTA^{Et}, thus called upon a further optimized procedure for the preparation of PCOE/PPG SMPs.

One-pot, two-step ROIMP of COE and PPG catalyzed by G2 and CM in the presence of CTA^{Et} - Method II.

First step: ROIMP of COE and PPG catalyzed by G2. All polymerizations were performed according to the following typical procedure (Scheme 1) (Table 1, entry 1). Under argon atmosphere, a Schlenk flask equipped with a magnetic stir bar, was charged sequentially with dry CH_2Cl_2 (5.0 mL), COE (0.5 g, 4.5 mmol) and tripropyleneglycol diacrylate PPG (0.45 g, 1.5 mmol). The initial concentration of COE/PPG was maintained at 0.5 $mol.L^{-1}$. The resulting solution was heated at 40 °C under a flow of argon and the polymerization was started upon addition, *via* a cannula, of a freshly prepared CH_2Cl_2 solution (1.0 mL) of G2 (2.5 mg, 3.0 μmol). The reaction mixture turned highly viscous within 2 min. The viscosity then slowly decreased over the following 10 min. After the desired reaction time (typically 2 h; reaction time was not necessarily optimized), an aliquot of the reaction medium was taken and the PCOE/PPG copolymer was characterized by 1D and 2D NMR spectroscopy, SEC and MS analyses (Figures S15–S19) (Table 1).

***Second step: CM of PCOE/PPG catalyzed by G2 in the presence of CTA^{Et}*.** All polymerizations were performed according to the following typical procedure (Scheme 1) (Table 2, entry 1). CTA^{Et} (180 mg, 0.30 mmol) was then added to the above reaction medium of PCOE/PPG in CH_2Cl_2 at 40 °C, and a freshly prepared CH_2Cl_2 solution (1.0 mL) of G2 (2.5 mg, 3.0 μmol) was introduced *via* a cannula. After the desired reaction time (typically 24 h; reaction time was not necessarily optimized), volatiles (solvent and ethylene) were removed under vacuum. The PCOE/PPG-$[Si(OEt)_3]_2$ copolymer was recovered without further purification, as a brownish viscous liquid (99%, 0.95 g) at 25 °C, which is readily soluble in $CHCl_3$ and THF. The isolated PCOE/PPG-$[Si(OEt)_3]_2$ copolymers was then characterized by 1D and 2D NMR spectroscopy, ESI-MS, SEC, and FT-IR analyses (Figures 1,S20–S24) (Table 2).

One-pot, one-step ROIMP/CM of COE and PPG* catalyzed by G2 in the presence of CTA^{Et}: Large-scale synthesis - Method I. All polymerizations were performed according to the following typical procedure, as previously reported (Table S7, entry 5).[4] Note that this approach is the same as the one described above with PPG ("One-pot, one-step ROIMP/CM of COE with PPG catalyzed by G2 in the presence of CTA^{Et}"), yet it is performed with PPG* and with some modified operating conditions. For a greener procedure, the large-scale metathesis reaction was performed in a concentrated medium ($[COE]_0$ + $[PPG*]_0$ = 6 M vs 0.5 M, Table S7, entries 4−6 vs entries 1−3) over a shorter reaction time (20 min vs 26 h). These operating conditions drastically reduced the amount of CH_2Cl_2 required (from 400 to 50 mL) and of G2 catalyst (from 750 to 200 mg for 100 g of copolymer), and enabled the large-scale synthesis of the copolymer (up to 100 g) in a single batch.

Typically, under an argon atmosphere, a Schlenk flask equipped with a magnetic stir bar was charged sequentially with CH_2Cl_2 (40.0 mL), COE (24.0 g, 218 mmol), PPG* (16.0 g, 6.7 mmol) and CTA^{Et} (6.4 g, 11.0 mmol). The resulting solution was heated at 40 °C and the polymerization was started upon addition, via a cannula, of a dry, freshly prepared CH_2Cl_2 solution (10.0 mL) of G2 (200 mg, 0.22 mmol). The reaction mixture turned highly viscous within 2 min. After 20 min, volatiles were removed under vacuum at 80 °C and the reaction mixture progressively turned liquid within 24 h. Also, the ethylene formed from the reaction of the acrylate and vinyl chain-ends was immediately flushed out either by a flow of argon of by vacuum. The copolymer was recovered without further purification (ca. 10 g), as a brownish viscous liquid at 25 °C, which is readily soluble in $CHCl_3$ and THF. To avoid possible issues of a single larger scale-up experiment of 100 g, 10 individual batches of 10 g each were prepared and ultimately combined to provide 100 g of copolymers (Table S7). The isolated

α,ω-$[(EtO)_3Si]_2$-PCOE/PPG* copolymers were characterized by ^{1}H and 2D NMR and FTIR spectroscopies, SEC, TGA, DSC, and rheological analyses.[4]

Theoretical molar mass determination of α,ω-$[Si(OEt)_3]_2$-PCOE/PPG,PPG* SMPs prepared by ROMP/CM/IM. Despite the complexity of the reaction mixture, of the mechanisms at play and of the resulting NMR spectra, a theoretical molar mass was proposed according to the following formula, as illustrated with PPG:

$$M_{n,theo} = \frac{([COE]_0 \times M_{COE} \times conv._{COE}) + ([PPG]_0 \times M_{PPG} \times conv._{PPG}) + ([\mathrm{CTAEt}]_0 \times M_{CTAEt} \times conv._{CTAEt})}{([PPG]_0 \times conv._{PPG} \times (1 - released_{ethylene})) + ([\mathrm{CTAEt}]_0 \times conv._{CTAEt})}$$

with $[X]_0$ = the initial concentration of compound X, M_X = the mass of compound X, $conv._X$ = the final conversion in compound X, $released_{ethylene}$ = the ratio of ethylene formed and released during the synthesis in comparison to the maximum possible. Noteworthy, in all our experiments, the $conv._{COE}$ reached 100%.

In this formula, we assumed that PPG acts both as a monomer and a CTA due to its ability to cleave the chains, but a factor ($1–released_{ethylene}$) was added to take into account the possibility to reform the chains by elimination of ethylene (Scheme S7). The formation of cyclic-non-functional chains is not taken in account is this formula because they cannot be distinguished from linear polymer chains by NMR spectroscopy. Previous work on the ROMP/CM process showed that they are formed generally in minor amounts (ca. 5−20%).[3,7-9]

Tensile testing of S1/G9 (1:1wt%)-cured SMPs - ***The procedure reminded thereafter was already reported.*****[4]** Adhesive tests were performed on all the SMPs listed in Table 3. The adhesive test consisted in the preparation of a wooden tensile piece, based on two pieces of wood bonded by a controlled amount of “glue” made from the cured SMPs. Typically, the α,ω-$[(EtO)_3Si]_2$-PCOE/PPG* copolymer and the catalytic system (1wt% S1 and 1wt% GF9) were mixed (at a temperature at which the SMP is liquid) in an aluminum cup (Figure S12 in ref 4, top left); then, the mixture was quickly poured onto a preheated wooden test piece, on a surface delimited by two Teflon blocks of 300 µm thickness (Figure S12 in ref 4, top right). Another wood test piece was counter-applied on the SMP and the two pieces were maintained together with pliers to form the tensile piece (Figure S12 in ref 4, bottom).

Finally, the SMPs were cured during 7 days at 25 °C under 44% of air-moisture. This tensile piece was then pulled out at rate of 10 $mm.min^{-1}$ by a traction machine, until break.

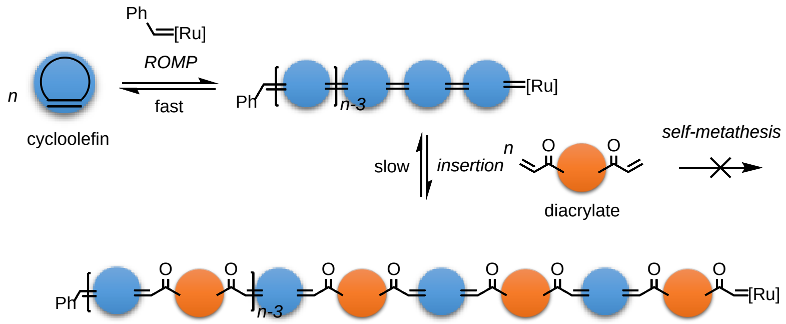

Scheme S1. Illustration of the ROIMP synthesis of an alternated copolymer from a cycloolefin and a diacrylate, as first established by Grubbs and co-workers.[1]

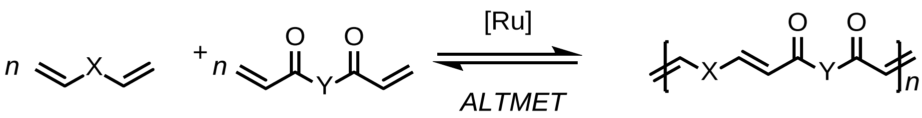

Scheme S2. ALTMET synthesis of alternated copolymers.[2]

It was reported that ALTMET does not require a low pressure and a high temperature to proceed efficiently, in contrast with ADMET, thanks to the thermodynamically favored bond formation between the diacrylate and diene.[2] However, a limitation of ALTMET is the need of relatively high loading in catalyst (generally 0.5−1 mol%) in comparison to conventional polymerization tools where ppm-levels are achieved. It is in fact well-documented that the CM reaction between olefins and acrylates requires a high catalyst loading [S. J. Langford, M. J. Latter, C. P. Woodward, *Org. Lett.* **2006**, *8*, 2595–2598; C. Lexer, R. Saf, C. Slugovc, *J. Polym. Sci. A1* **2009**, *47*, 299–305 ; S. Fustero, M. Sánchez-Roselló, J. F. Sanz-Cervera, J. L. Aceña, C. del Pozo, B. Fernández, A. Bartolomé, A. Asensio, *Org. Lett.* **2006**, 8, 4633–4636]. Later on, Slugovc *et al.* screened several olefin metathesis catalysts and reaction conditions to overcome this limitation and reached loadings as low as 0.1 mol% with Grubbs' second generation catalyst **G2** and Hoveyda-Grubbs catalyst **HG2** at 80 °C without solvent [[2]; M. Abbas, C. Slugovc, *Tet.Lett.* **2011**, *52*, 2560–2562]. Yet, these conditions are not suitable for metathesis polymerization methods that generally require low boiling point solvents to solubilize the reagents and products.

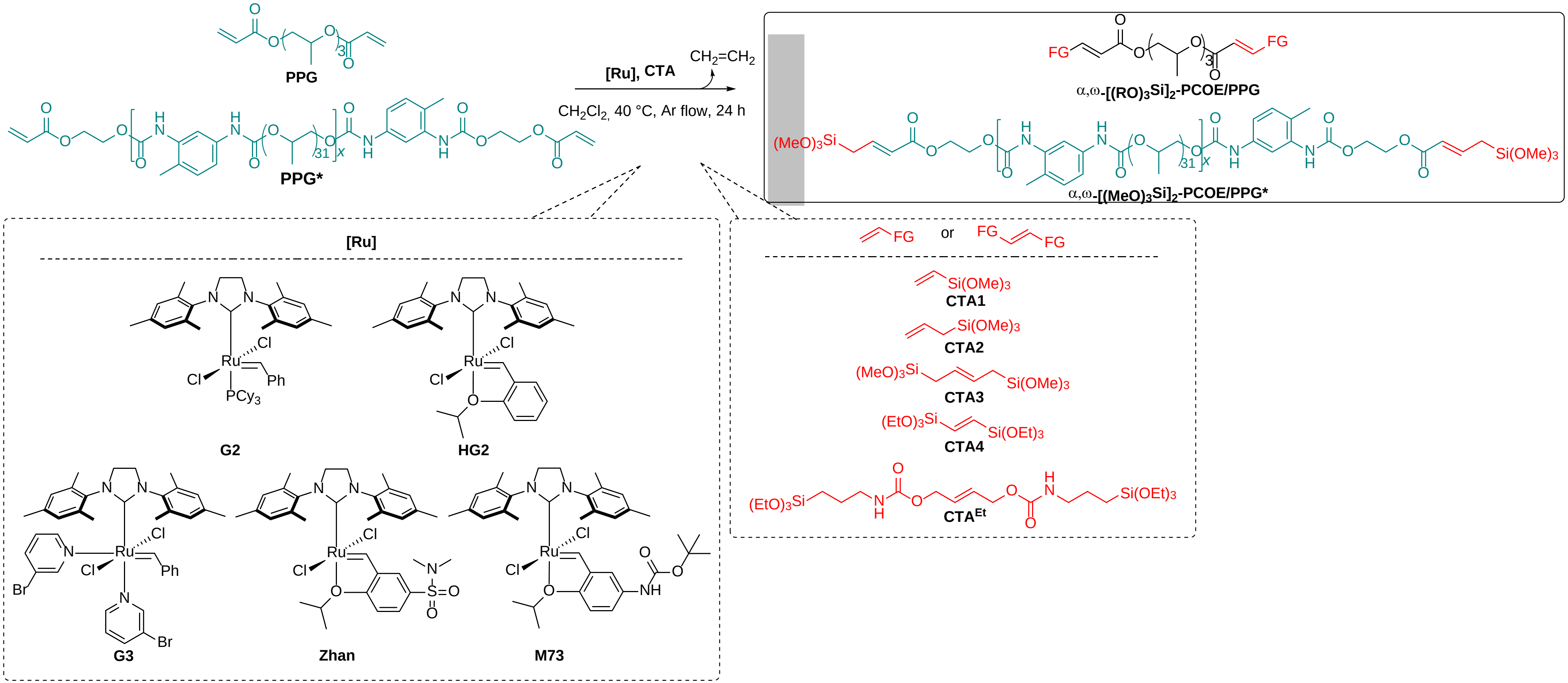

Scheme S3. Synthesis of PPG- and PPG*-based SMPs by CM of PPG and PPG*, respectively, using various catalysts in the presence of a trialkoxysilyl CTA.

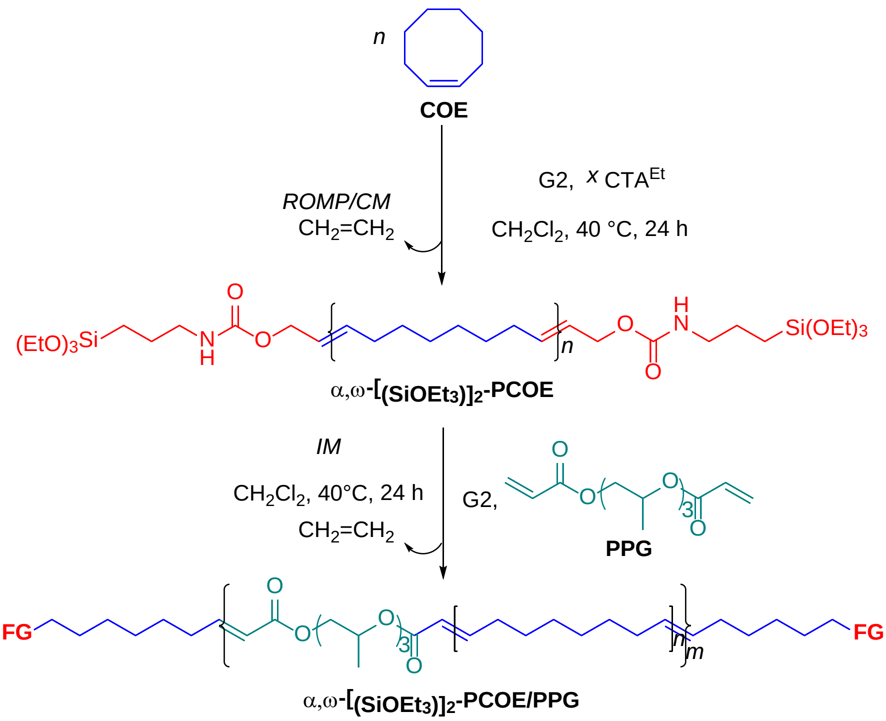

Scheme S4. Synthesis of α,ω-$[Si(OEt)_3]_2$-PCOE/PPG by the sequential (one-pot or two-pot) two-step ROMP/CM of COE catalyzed by G2 in the presence of CTA^{Et} [3]and the subsequent IM of PPG.

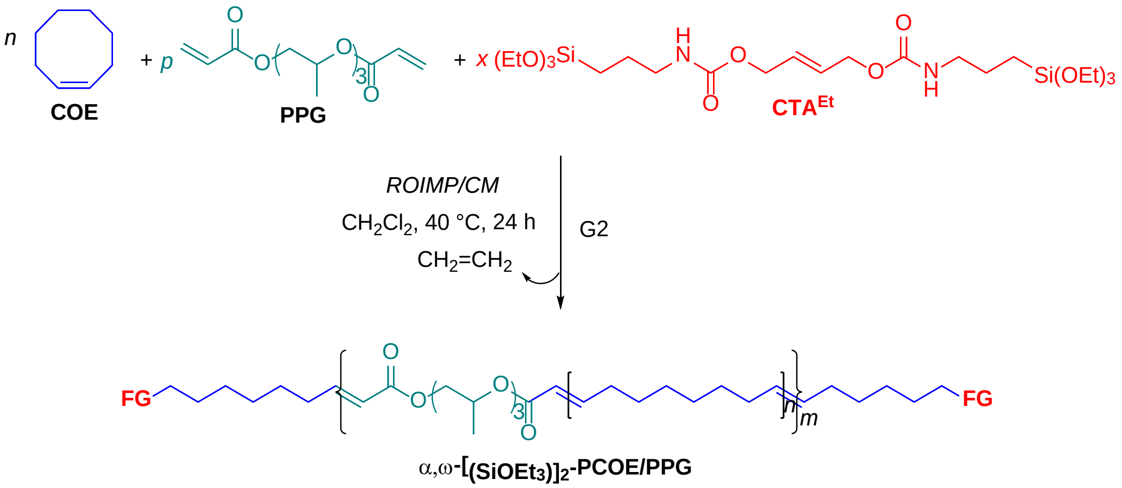

Scheme S5. Synthesis of α,ω-$[Si(OEt)_3]_2$-PCOE/PPG by the one-pot, one-step ROIMP of COE with PPG / CM with CTA^{Et} catalyzed by G2 – Method I, as previously established with PPG*.[4]

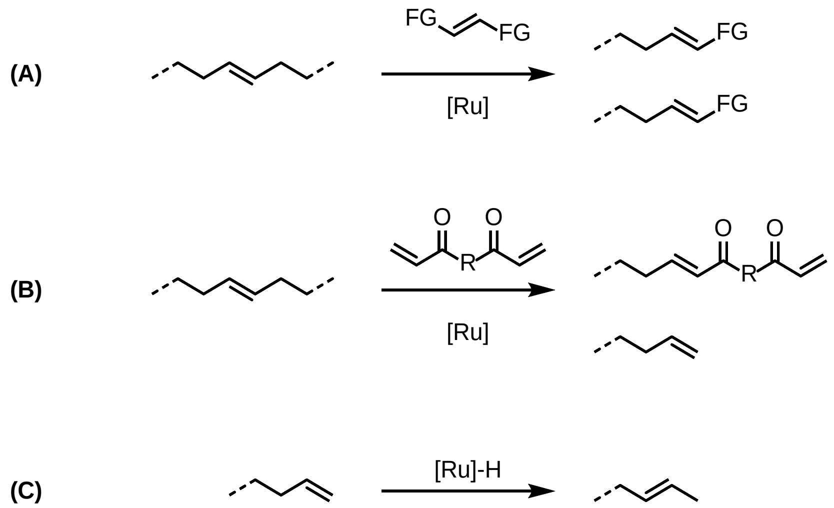

Scheme S6. Formation of the four different chain-ends upon metathesis polymerization reactions (A: trialkoxysilyl, B: acrylate and vinyl, C: isomerized, chain-end groups) during the metathesis processes.

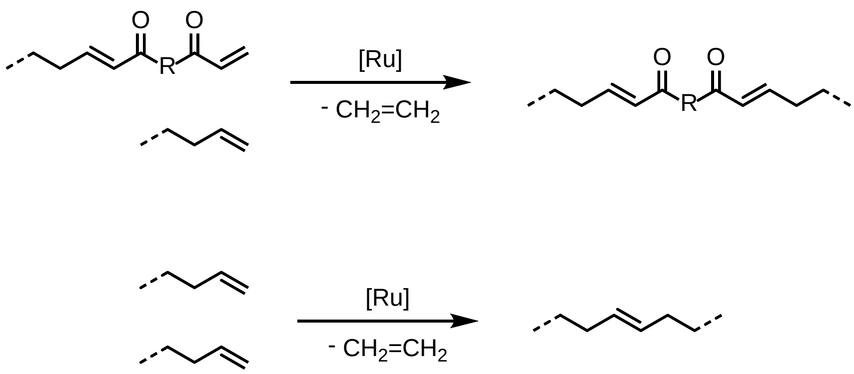

Scheme S7. Formation of ethylene during the ROIMP/CM process.[5]

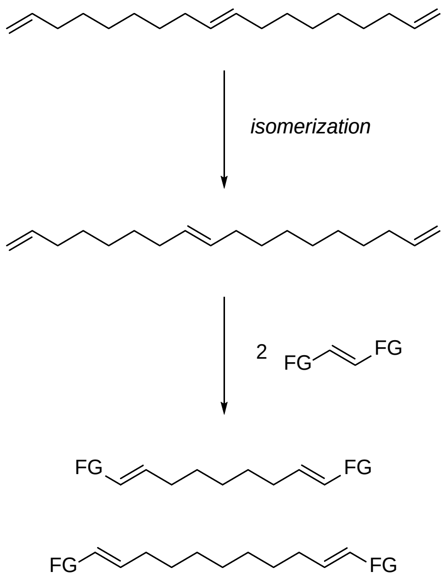

Scheme S8. Illustration of the formation of polymer chains with a missing or an additional CH_2 during the CM of PCOE/PPG with the CTA (FG: trialkoxysilyl functional group).

Table S1. Literature examples of ROIMP polymers, their A,B-alternations, molar mass values, and dispersities.[1]

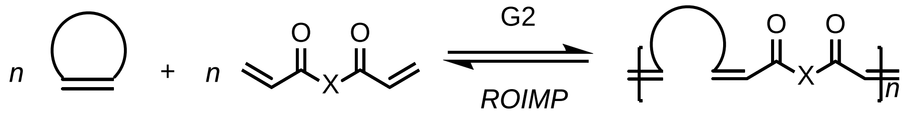

Entry	Diacrylate	Cycloolefin[a]	$[M]_0:[G2]_0$[b]	$[\text{diacrylate}]_0$[c] (mol/L)	Yield[d] (%)	Alternation[e] (%)	M_n[f] (g/mol)	$Đ_M$[f]
1	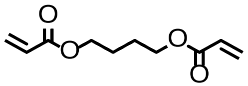	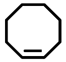	290:1	0.2	84	84	90 000	1.7
2	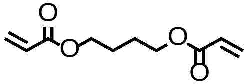		125:1	0.4	75	96	20 300	1.6
3	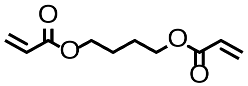	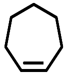	125:1	0.4	93	97	14 000	1.8
4	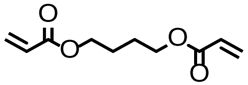	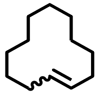	200:1	0.4	91	94	26 100	1.7
5	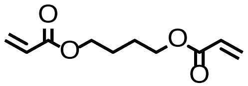	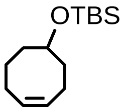	250:1	0.4	69	94.5	21 400	1.4
6	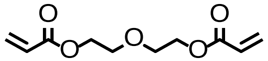	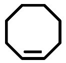	200:1	0.2	99	98.5	26 500	1.8
7	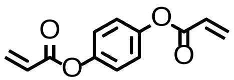	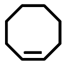	100:1	0.1	98	97	25 200	2.1

[a] 1.0 equivalent of cycloolefin was used, except for cyclopentene (1.3 equiv). [b] Total monomer:catalyst ratio. [c] Concentration with respect to diacrylate. [d] Yields of isolated products after precipitation into hexane or methanol. [e] Determined by ^{1}H NMR spectroscopic analysis. [f] Determined by SEC performed in CH_2Cl_2 relative to polystyrene standards.

Table S2. CM of PPG catalyzed by various ruthenium catalysts using several CTAs (Scheme S3).[a]

Entry	CTA[b]	Catalyst[c]	$[PPG]_0/[CTA]_0/[Cat.]_0$	Acrylate Conv.[d] (%)
1	CTA1	G2	200:450:1	23
2	CTA2	G2	200:450:1	98
3	CTA3	G2	200:225:1	92
4	CTA4	G2	200:225:1	0
5	CTA^{Et}	G2	200:225:1	0
6	CTA2	G2[e]	3000:7000:1	70
7	CTA2	G2[e]	3000:7000:1	78
8	CTA2	HG2[e]	3000:7000:1	92
9	CTA2	HG2[e]	3000:7000:1	88
10	CTA2	G3[e]	3000:7000:1	30
11	CTA2	G3[e]	3000:7000:1	38
12	CTA2	Zhan[e]	3000:7000:1	41
13	CTA2	Zhan[e]	3000:7000:1	40
14	CTA2	M73[e]	3000:7000:1	43
15	CTA2	M73[e]	3000:7000:1	46

[a] Reaction conditions: CH_2Cl_2, 40 °C, 24 h (non-optimized reaction time), under Ar flow. [3,7-9] [b] CTA1 and CTA2 are commercially available and were used after distillation under reduced pressure. CTA3, CTA4 and CTAEt were synthesized as previously described.[3,4,7-9] [c] HG2: Hoveyda-Grubbs' second generation catalyst; G2: Grubbs' second generation catalyst; G3: Grubbs' third generation catalyst; Zhan: Zhan catalyst-1B; M73: Umicore catalyst M73-SiPr. [d] Determined by ^1H NMR spectroscopy (refer to the Experimental Section). [e] Sequential addition of the catalyst in three fractions over 2 h.

Table S3. CM of PPG* catalyzed by G2 using CTA2 (Scheme S3).[a]

Entry	Catalyst	m_{PPG*} (g)	$[PPG^*]_0/[CTA2]_0/[G2]_0$	Acrylate Conv.[b] (%)
1	G2	2.2	200:420:1	96
2	G2 [c]	22.5	133:280:1	97
3	G2 [c]	22.5	133:280:1	88
4	G2 [c]	22.5	133:280:1	88
5	G2 [c]	22.5	133:280:1	88
6[d]	-	90	-	97

[a] Reaction conditions: CH_2Cl_2, 40 °C, 24 h (non-optimized reaction time), under Ar flow[3,7-9] [b] Determined by ^1H NMR spectroscopy (refer to the Experimental Section). [c] Sequential addition in five fractions over 2 h. [d] Blend of samples isolated from entries 2–5, after distillation under vacuum at 70 °C for 2 h.

Table S4. ROMP/CM of COE

catalyzed by G2 in the presence of CTA^{Et} in CH_2Cl_2 at 40 °C during 24 h (Scheme S4).

Entry	$[COE]_0/[G2]_0/[CTA^{Et}]_0$ [a]	$Conv._{CTAEt}$ [b] (%)	$M_{n,theo}$ [c] ($g.mol^{-1}$)	$M_{n,SEC}$ [d] ($g.mol^{-1}$)	$Đ_M$ [d]	Table S5
1	2000:1:100	95	2700	*n.d.*	*n.d.*	Used *in situ*
2	2000:1:100	96	2300	5000	2.0	Used *in situ*
3	2000:1:100	95	2300	4700	2.1	Isolated

[a] Reaction performed under a flow of argon to remove the ethylene released; $[COE]_0$ = 1.8 $mol.L^{-1}$, $[G2]_0$ = 5.9 µmol 0.05 mol%; reaction time was not optimized; 100 % conversion in COE as determined by ^1H NMR analysis (refer to the Experimental Section). [b] Determined by ^1H NMR analysis). [c] Theoretical molar mass value calculated from the formula: $M_{n,theo} = \{([COE]_0 \times conv._{COE} \times M_{COE}) / ([CTA^{Et}]_0 \times Conv._{CTAEt} \times M_{CTA})\}$, with M_{COE} = 110 $g.mol^{-1}$, M_{CTAEt} = 582 $g.mol^{-1}$, based on the formation of only difunctional PCOE (i.e. without considering any cyclic PCOE).[3] [d] Number-average molar mass ($M_{n,SEC}$) and dispersity ($Đ_M = M_w/M_n$) values determined by SEC vs polystyrene standards in THF at 30 °C. *n.d.* not determined.

Table S5. IM of PPG into α,ω-$[Si(Et)_3]_2$-PCOE prepolymer catalyzed by G2 in CH_2Cl_2 at 40 °C during 24 h (Scheme S4).

Entry	$[Si(OEt)_3]_2$-PCOE (Table S4)	$[Si(OEt)_3]_2$-PCOE]$_0$/[PPG]$_0$ [a]	[G2]$_0$ [a]	Conv.$_{acrylate}$ [b] (%)	Released ethylene [b] (%)	Chain-end ratio [b]				$M_{n,theo}$ [c] (g.mol^{-1})	$M_{n,SEC}$ [d] (g.mol^{-1})	$Đ_M$ [d]
						Acryl.	Si(OE*t*)$_3$	Vinyl	Isom.			
1	Entry 1 [e]	1500:500	2	29	15	65	12	13	9	1350	1500[f]	1.7
2	Entry 2 [e]	1500:500	1/+10	23/50	32/45	54	15	18	13	1400	2000[f]	2.0
3	Entry 3 [g]	1500:500	10	78	77	48	14	20	18	2000	3300[f]	1.7
4	Entry 3 [g]	1500:500	1/+1/+10	32/36/58	20/34/63	60	9	2	29	1600	2100[f]	2.0
5	Entry 3 [g]	1500:500	1+1/+2+2/+2+2+2	40/53/60	50/32/74	64	11	8	16	1900	2600[f]	2.1

[a] Reaction performed under a flow of argon to remove the ethylene releazed; $[COE]_0+[PPG]_0$ = 0.5 M; reaction time was not optimized; 100 % conversion in COE as determined by ^{1}H NMR analysis (refer to the Experimental Section). [b] Determined by ^{1}H NMR analysis. [c] Theoretical molar mass value calculated from the formula: $M_{n,theo} = \{([COE]_0 \times conv._{COE} \times M_{COE}) + ([PPG]_0 \times Conv._{PPG} \times M_{PPG}) + ([CTA^{Et}]_0 \times conv._{CTAEt} \times M_{CTAEt})\} / \{([PPG]_0 \times conv._{PPG} \times (1 - \text{released ethylene})) + ([CTA^{Et}]_0 \times conv._{CTAEt})\}$ (refer to the Supporting Information), with M_{COE} = 110 g.mol^{-1}, M_{PPG} = 300 g.mol^{-1}, M_{CTAEt} = 582 g.mol^{-1}. [d] Number-average molar mass ($M_{n,SEC}$) and dispersity ($Đ_M = M_w/M_n$) values determined by SEC vs polystyrene standards in THF at 30 °C. [e] Prepolymer used *in situ*. [f] A population at 140 g.mol^{-1} corresponding to unreacted PPG was also observed in all experiments, possibly due to the catalyst deactivation. [f] Prepolymer isolated prior to the IM reaction.

Table S6. One-pot, one-step ROIMP of COE with PPG and CM with CTA^{Et} catalyzed by G2 in CH_2Cl_2 at 40 °C during 24 h (Scheme S5).

Entry	$[COE]_0/[PPG]_0/[CTA^{Et}]_0$ [a]	[G2]$_0$	Conversion [b] (%)		Released ethylene [b] (%)	Chain-end ratio [b]				$M_{n,theo}$ [c] (g.mol^{-1})	$M_{n,SEC}$ [d] (g.mol^{-1})	$Đ_M$ [d]
			CTA^{Et}	Acrylate		Acryl.	Si(OEt)$_3$	Vinyl	Isom.			
1	1500:500:100	1+10	94	34	26	65	10	1	24	1350	2400[e]	2.0
2	1500:500:100	10	88	52	44	53	14	16	17	1350	2200[e]	1.9
3	1500:500:100	2	75	38	5	56	11	17	16	1100	1500[e]	1.7

[a] Reaction performed under a flow of argon to remove the ethylene released; $[COE]_0+[PPG]_0$ = 0.5 M; reaction time was not optimized; 100 % conversion in COE as determined by ^{1}H NMR analysis (refer to the Experimental Section). [b] Determined by ^{1}H NMR analysis. [c] Theoretical molar mass value calculated from the formula: $M_{n,theo} = \{([COE]_0 \times conv._{COE} \times M_{COE}) + ([PPG]_0 \times Conv._{PPG} \times M_{PPG}) + ([CTA^{Et}]_0 \times conv._{CTAEt} \times M_{CTAEt})\} / \{([PPG]_0 \times conv._{PPG} \times (1 - \text{released ethylene})) + ([CTA^{Et}]_0 \times conv._{CTAEt})\}$ (refer to the Supporting Information), with M_{COE} = 110 g.mol^{-1}, M_{PPG} = 300 g.mol^{-1}, M_{CTAEt} = 582 g.mol^{-1}. [d] Number-average molar mass ($M_{n,SEC}$) and dispersity ($Đ_M = M_w/M_n$) values determined by SEC vs polystyrene standards in THF at 30 °C. [e] A population at 140 g.mol^{-1} corresponding to unreacted PPG was also observed.

Table S7. Large-scale ROIMP/CM of PCOE and PPG* catalyzed by G2 in the presence of CTA^{Et} (Scheme S5).[a]

Entry	Scheme (Method)[a]	Polymer [b]	$[COE]_0/[PPG^*]_0/[CTA^{Et}]_0/[G2]_0$	$w_{COE}/w_{PPG*}/w_{CTAEt}$ [c]	Conv.[d] (%)		Released ethylene[d] (%)	Chain-end ratio[d]				$M_{n,theo}$[e] (g.mol^{-1})	$M_{n,SEC}$[f] (g.mol^{-1})	$Đ_M$[f]
					CTA	Acryl.		Acryl.	$Si(OEt)_3$	Vinyl	Isom.			
0	-	α,ω-$[(EtO)_3Si]_2$-PCOE [3]	100:0:1:0.05	95:0:5	99	-	-	-	100	0	0	11000	18 500	2.1
1	1 (II[g])	$PCOE^{20}/PPG^{*65}-CTA^{Et15}$	8.0:1.09:1:0.06	20:65:15	89	98	75	3	70	4	24	3500	14 000	2.1
2	1 (II[g])	$PCOE^{35}/PPG^{*50}-CTA^{Et15}$	13.4:0.86:1:0.06	35:50:15	100	97	61	2	73	5	19	3200	12 400	2.5
3	1 (II[g])	$PCOE^{50}/PPG^{*35}-CTA^{Et15}$	19.4:0.60:1:0.06	50:35:15	99	97	58	1	68	6	25	3500	12 500	2.5
4 [4]	- [4] (I)	$PCOE^{47}/PPG^{*31}-CTA^{Et22}$	11.7:0.36:1:0.01	47:31:22	91	89	16	4	68	14	14	2400	9700	2.1
5 [4]	-[4] (I)	$PCOE^{50}/PPG^{*35}-CTA^{Et15}$	19.4:0.60:1:0.02	50:35:15	93	96	19	4	58	19	20	3000	13 000	2.1
6 [4]	-[4] (I)	$PCOE^{56}/PPG^{*37}-CTA^{Et7}$	41.3:1.27:1:0.04	56:37:7	100	100	11	0	41	20	39	3900	18 300	2.1

[a] Reaction conditions: CH_2Cl_2, 40 °C, under a flow of argon. Refer to the Experimental Section. [b] SMPs referred to as $PCOE^x/PPG^{*y}-CTA^z$ (with x, y, z = weight fraction of PCOE, PPG*, and alkoxysilyl chain end-groups, respectively, x+y+z = 100wt%). [c] Mass ratio. [d] Determined by ^1H NMR spectroscopy; note that the amount of ethylene is underestimated. [e] Theoretical molar mass calculated from the formula: $M_{n,theo} = \{([COE]_0 \times M_{COE} \times conv._{COE}) + ([PPG^*]_0 \times M_{PPG^*} \times conv._{PPG^*}) + ([CTA]_0 \times M_{CTA} \times conv._{CTA})\} / \{([PPG^*]_0 \times conv._{PPG^*} \times (1 - released_{ethylene})) + ([CTA]_0 \times conv._{CTA})\}$, with M_{COE} = 110 g.mol^{-1}, M_{PPG^*} = 2400 g.mol^{-1}, M_{CTAEt} = 582 g.mol^{-1} and M_{CTAMe} = 498 g.mol^{-1}. Quantitative COE conversion as determined by ^1H NMR analysis. [f] Number-average molar mass ($M_{n,SEC}$) and dispersity ($Đ_M = M_w/M_n$) values determined by SEC vs polystyrene standards in THF at 30 °C (uncorrected M_n values; Figure S25). [g] Large-scale synthesis.

Three different $[COE]_0/[PPG^*]_0$ ratios were used (maintaining the CTA^{Et}/G2 loading ratio constant) to probe the effect of the PCOE content within the copolymer on the final material properties (Table S7 entries 1−3). High acrylate (ca. 97%) and CTA^{Et} (89−100%) conversions were obtained and a fair-to-good release of ethylene (58−75%) was measured. High triethoxysilyl end-group incorporation (68−73%), and high extent of isomerization were observed (Vinyl/Isom. = 0.16−0.26), while relatively high $M_{n,SEC}$ values (12 400−14 000 g.mol^{-1}) were measured. NMR and FT-IR analyses of the sample thus recovered supported the formation of the expected PCOE/PPG*-$[Si(OEt)_3]_2$ alternated copolymer.[4]

Table S8. Thermal characteristics of α,ω-$[(EtO)_3Si]_2$-PCOE/PPG* SMPs prepared from the direct simpler tandem ROIMP/CM (one-pot, one-step) route – Method I (Table S7).[4]

Entry	Polymer	$T_d^{10\%}$ [a] (°C)	$T_d^{20\%}$ [a] (°C)	T_g [b] (°C)	T_c [b] (°C)	T_m [b] (°C)	ΔH_{cryst} [b] ($J.g^{-1}$)
1	$PCOE^{50}/PPG^{*35}$-CTA^{Et15}	280	367	−54	40	55	−15
2	$PCOE^{56}/PPG^{*37}$-CTA^{Et7}	312	379	−48	40	55	−7
3	$PCOE^{47}/PPG^{*31}$-CTA^{Et22}	270	325	n.o.	40	55	−15

[a] Degradation temperatures determined by TGA with T_d^x = temperature at which x% of mass loss occurs (refer to Supporting Information). [b] Glass transition (T_g), crystallization (T_c) and melting (T_m) temperatures, and crystallization enthalpy (ΔH_{cryst}) determined by DSC (refer to the Supporting Information).

Table S9. Rheological characteristics of the α,ω-$[(EtO)_3Si]_2$-PCOE/PPG* SMPs prepared from the direct simpler tandem ROIMP/CM (one-pot, one-step) route – Method I (Table S7).[4]

Entry	SMP	T = 30 °C [a]			T = 60 °C [a]		
		$\eta^{\gamma=0.1}$ (Pa.s)	$\eta^{\gamma=100}$ (Pa.s)	Rheological behavior	$\eta^{\gamma=0.1}$ (Pa.s)	$\eta^{\gamma=100}$ (Pa.s)	Rheological behavior
1	$PCOE^{50}/PPG^{*35}$-CTA^{Et15}	7200	265	Rheofluidifying	6	5	Newtonian
2	$PCOE^{56}/PPG^{*37}$-CTA^{Et7}	8500	148	Rheofluidifying	33	12	Newtonian
3	$PCOE^{47}/PPG^{*31}$-CTA^{Et22}	3000	245	Rheofluidifying	5	3	Newtonian

[a] Viscosity and rheological behavior as determined by viscosimetry using a Contraves Low Shear 30 viscosimeter; uncertainty = ±5% (refer to Supporting Information). [b] Not determined because the polymer is solid. [c] Not determined because the viscosity at 30 °C was too high for our apparatus to measure it. n.o. not observed.

Table S10. Rheological data of α,ω-[$(EtO)_3Si]_2$-PCOE/PPG* SMPs synthesized by the one-pot, two-step ROIMP/CM route – large-scale synthesis (Method II) (Table S7).

η (Pa.s) \ γ (s^{-1})	**PPG* 30°C**	η (Pa.s) \ γ (s^{-1})	**PCOE[50]/PPG*[35]-CTA[Et15] 30°C**	**PCOE[35]/PPG*[50]-CTA[Et15] 30°C**	**PCOE[20]/PPG*[65]-CTA[Et15] 30°C**	**PCOE[50]/PPG*[35]-CTA[Et15] 60°C**	**PCOE[35]/PPG*[50]-CTA[Et15] 60°C**	**PCOE[20]/PPG*[65]-CTA[Et15] 60°C**	η (Pa.s) \ γ (s^{-1})	**Polyvest E100 30°C**
0,0172698	130,413	0,0172243	454034	293764	175536	15,0369			0,0172922	14,3764
0,029633	93,6882	0,0295948	282073	148446	101089	17,5576	1,38243		0,0297011	11,1528
0,0508654	71,3891	0,0508222	175577	73865,3	63078,6	18,4135	2,51948	3,00375	0,0510138	9,31102
0,0873486	57,5074	0,0873178	98540,5	41256,4	41032,1	18,3749	3,06324	4,02376	0,0876179	9,46238
0,150112	50	0,149879	50678,9	24726,7	26616	17,2226	3,40042	3,90316	0,15049	8,83728
0,257839	46,0694	0,25734	29493,6	15417,7	17129,8	15,7832	3,48374	4,37574	0,258503	8,37514
0,44287	42,949	0,441938	17932,1	9819,91	10841,4	14,1095	3,35714	4,31426	0,444021	8,03482
0,760876	40,4516	0,758976	10992,7	6301,52	6712,4	12,9042	3,20079	4,08818	0,762678	7,61849
1,3075	38,4933	1,30338	6796,33	3990,57	3999,7	11,9199	3,02436	4,04034	1,31002	7,51884
2,246	37,19	2,23827	4053,54	2386,19	2034,32	11,1119	2,91095	3,91333	2,25024	7,44608
3,85771	36,3657	3,84381	2520,24	1383,69	974,526	10,4233	2,76366	3,85354	3,86521	7,43684
6,62578	35,8269	6,60233	1572,23	854,02	382,367	9,91568	2,68378	3,79062	6,63922	7,41681
11,3809	35,2598	11,3397	1030,6	564,234	190,892	9,50094	2,68188	3,73597	11,4043	7,37823
19,5483	34,7506	19,477	788,841	378,216	118,963	9,10972	2,69351	3,6729	19,5885	7,36817
33,5779	34,2767	33,458	587,16	253,61	63,7482	8,61247	2,7395	3,60666	33,646	7,354
57,6758	33,7212	57,4826	427,02	185,679	41,7885	8,02846	2,78761	3,54472	57,7895	7,34043
99,0687	33,0864	98,7849	269,028	130,881	21,0876	7,65617	2,81515	3,44804	99,2567	7,32603
170,176	32,181	169,811	143,801	82,8802	16,0367	6,95933	2,82238	3,28866	170,608	7,2931
292,369	30,4184	292,034	92,7083	49,1038	19,2575	5,33745	2,79929	3,28304	293,377	7,22086
467,042	27,2431	467,555	49,2667	22,5387	9,78357		2,73441	3,01153	468,55	7,07429

Table S11. T_g and *E'* values measured by DMA analysis of S1/GF9(1:1wt%)-cured α,ω-[(EtO)$_3$Si]$_2$-PCOE/PPG* SMPs prepared in the present work from the tandem ROIMP/CM (one-pot, two-step) route – large-scale synthesis Method II (Table S7).

Entry	**SMPs**	T_g [a] (°C)	***E'* (MPa)**		
			Glassy plateau	**1st rubbery plateau**	**2nd rubbery plateau**
1	Polyvest E100	−70	2000	8.4	-
2	PCOE^{20}/PPG*^{65}-CTA^{Et15}	−40	1500	3.2	1.6
3	PCOE^{35}/PPG*^{50}-CTA^{Et15}	−43	3100	13.7	8.7
4	PCOE^{50}/PPG*^{35}-CTA^{Et15}	−43	2600	32.8	22.0

[a] Note that the glass transition temperature determined by DMA was more positive, as expected, than that obtained from DSC analyses (Table 3).

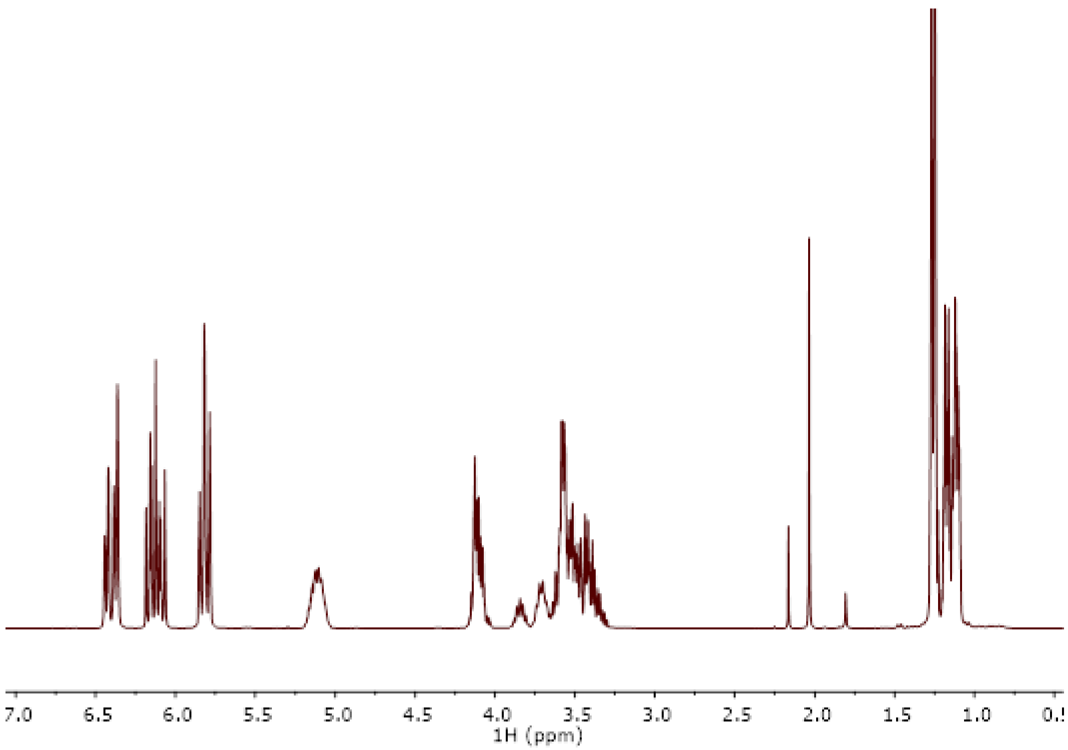

Figure S1. ^{1}H NMR spectrum (400 MHz, $CDCl_3$, 293 K) of PPG.

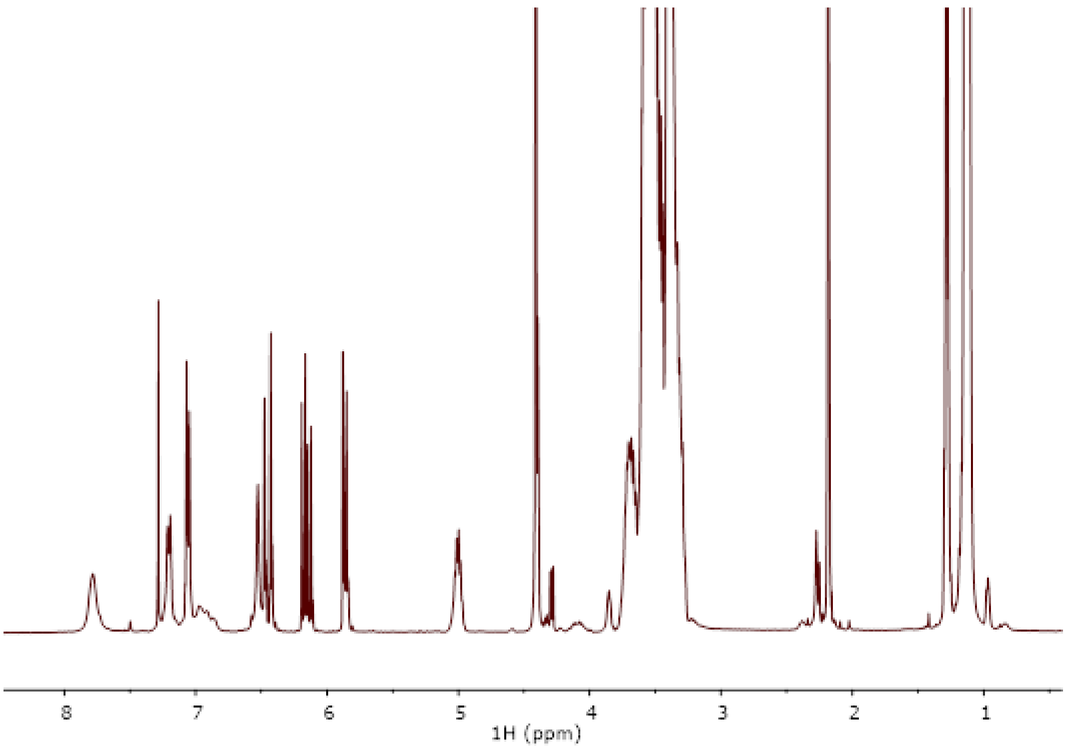

Figure S2. ^{1}H NMR spectrum (400 MHz, $CDCl_3$, 293 K) of PPG*.

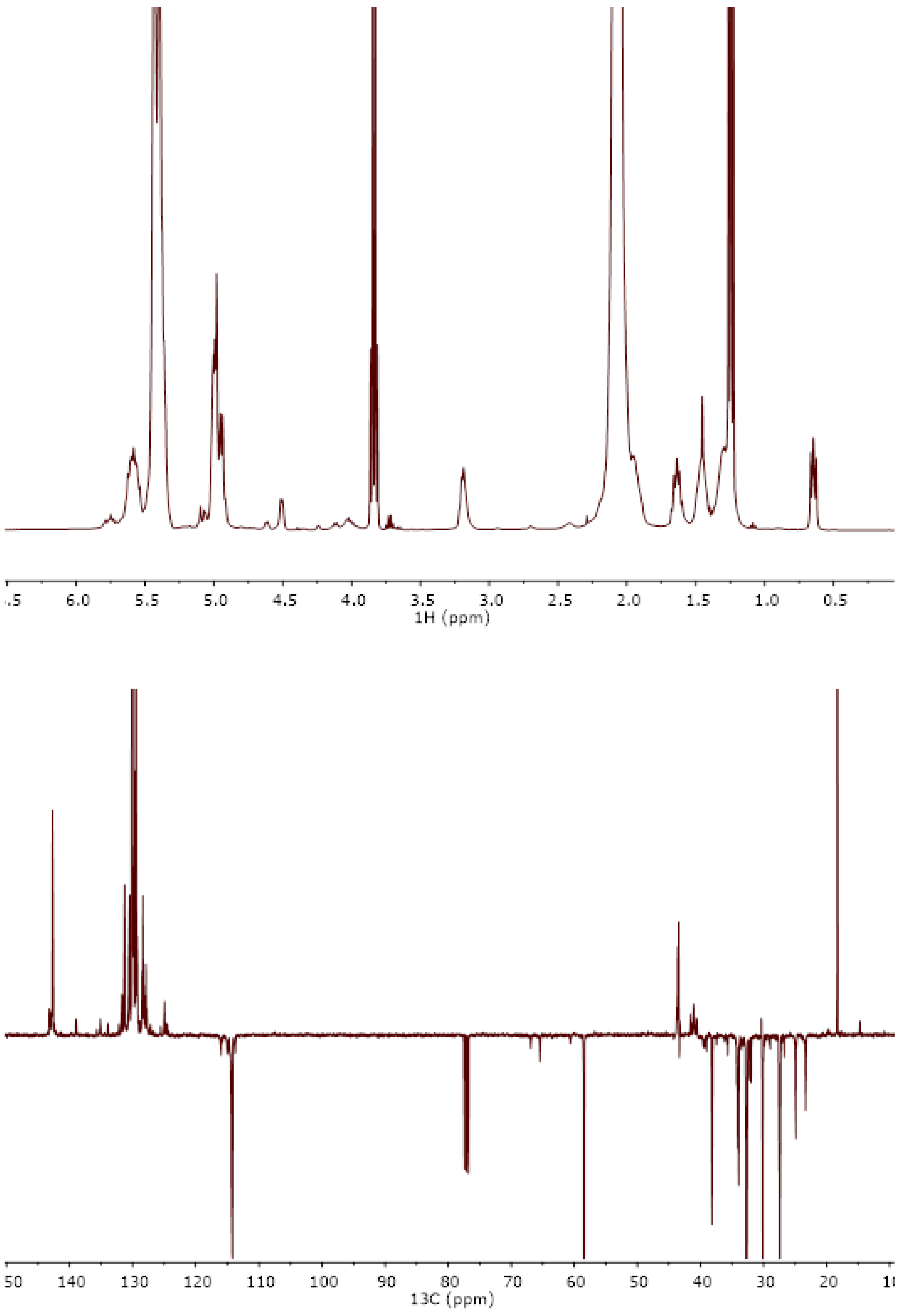

Figure S3. ^{1}H and J-MOD (400 and 100 MHz, $CDCl_3$, 293 K) NMR spectra of Polyvest E100.

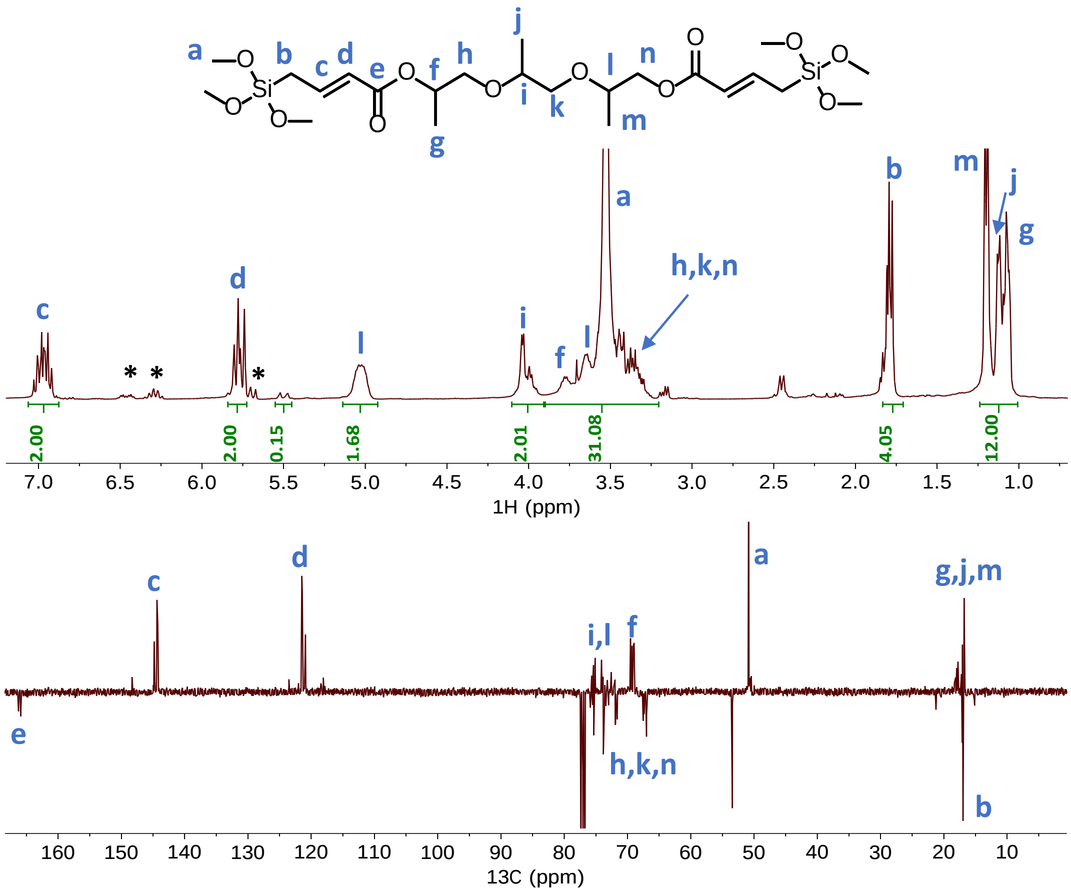

Figure S4. [1]H and J-MOD NMR spectra (400 and 100 MHz, 298 K, $CDCl_3$) of PPG-CTA2$_2$ isolated from the CM of PPG catalyzed by G2 using CTA2 (Table S2, entry 2); *: residual PPG-acrylate.

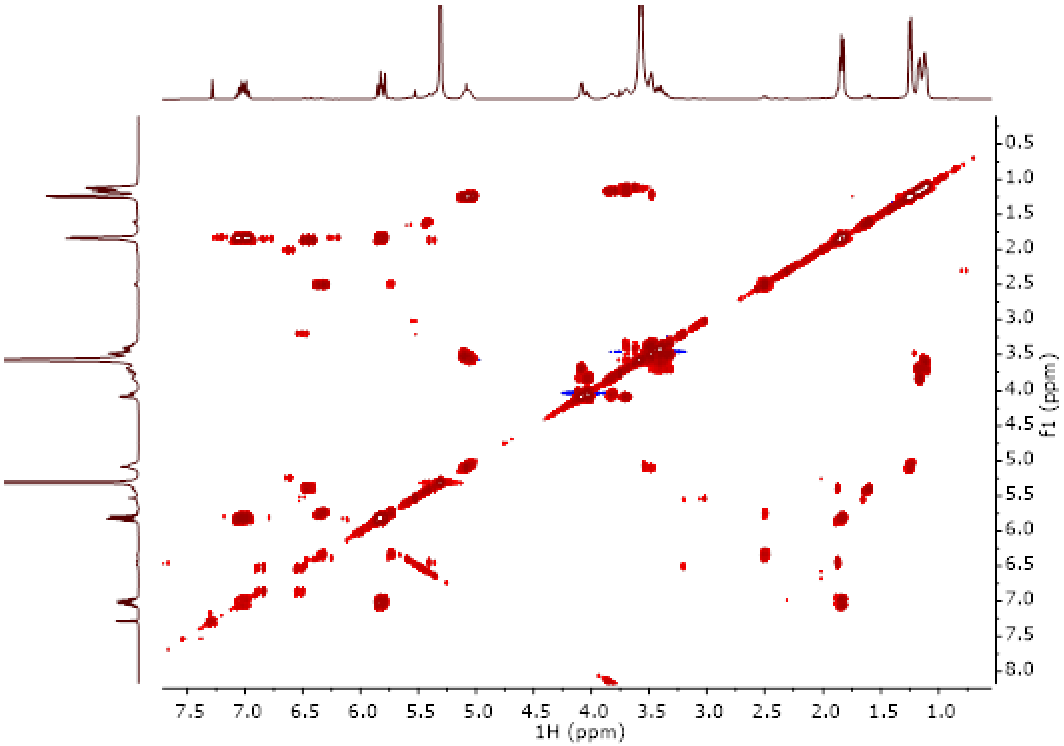

Figure S5. COSY NMR spectrum (400 MHz, $CDCl_3$, 293 K**)** of PPG-CTA2_2 isolated from the CM of PPG catalyzed by G2 using CTA2 (Table S2, entry 2).

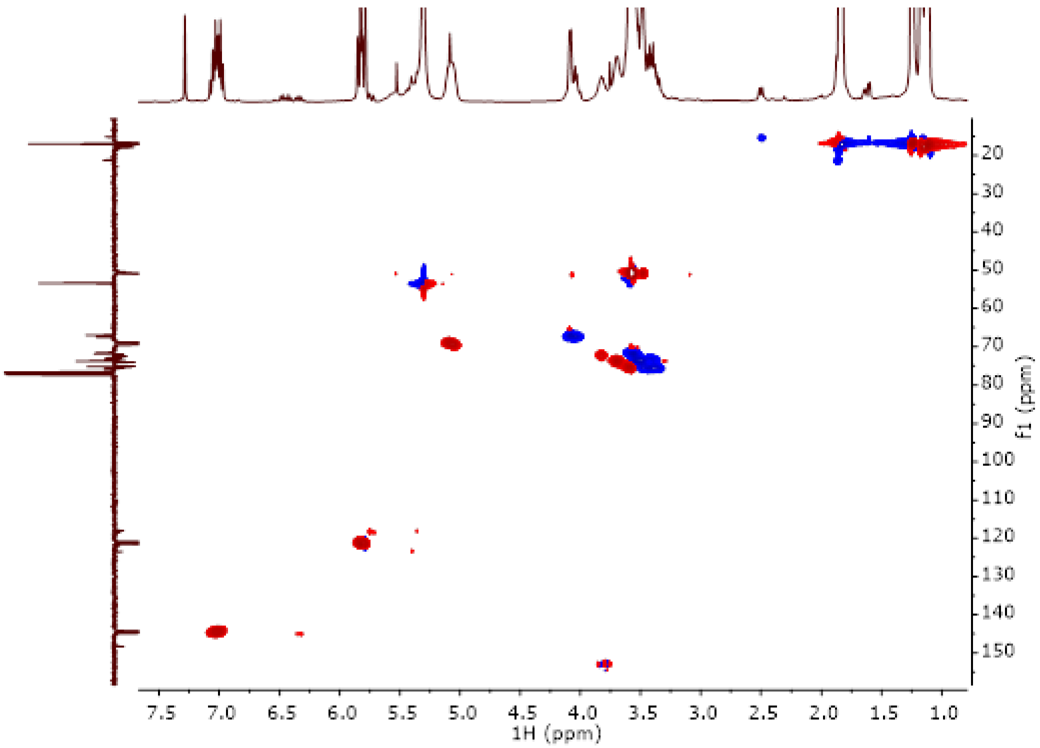

Figure S6. HSQC NMR spectrum (100 & 400 MHz, $CDCl_3$, 293 K**)** of PPG-CTA2_2 isolated from the CM of PPG catalyzed by G2 using CTA2 (Table S2, entry 2).

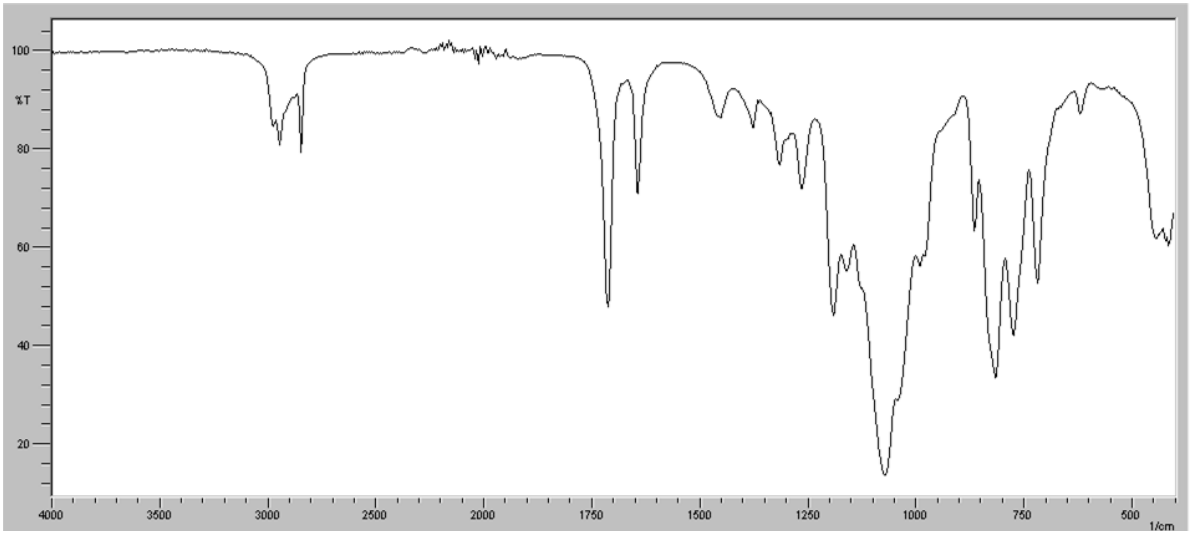

Figure S7. FT-IR spectrum of PPG-CTA2_2 isolated from the CM of PPG catalyzed by G2 using CTA2 (Table S2, entry 2).

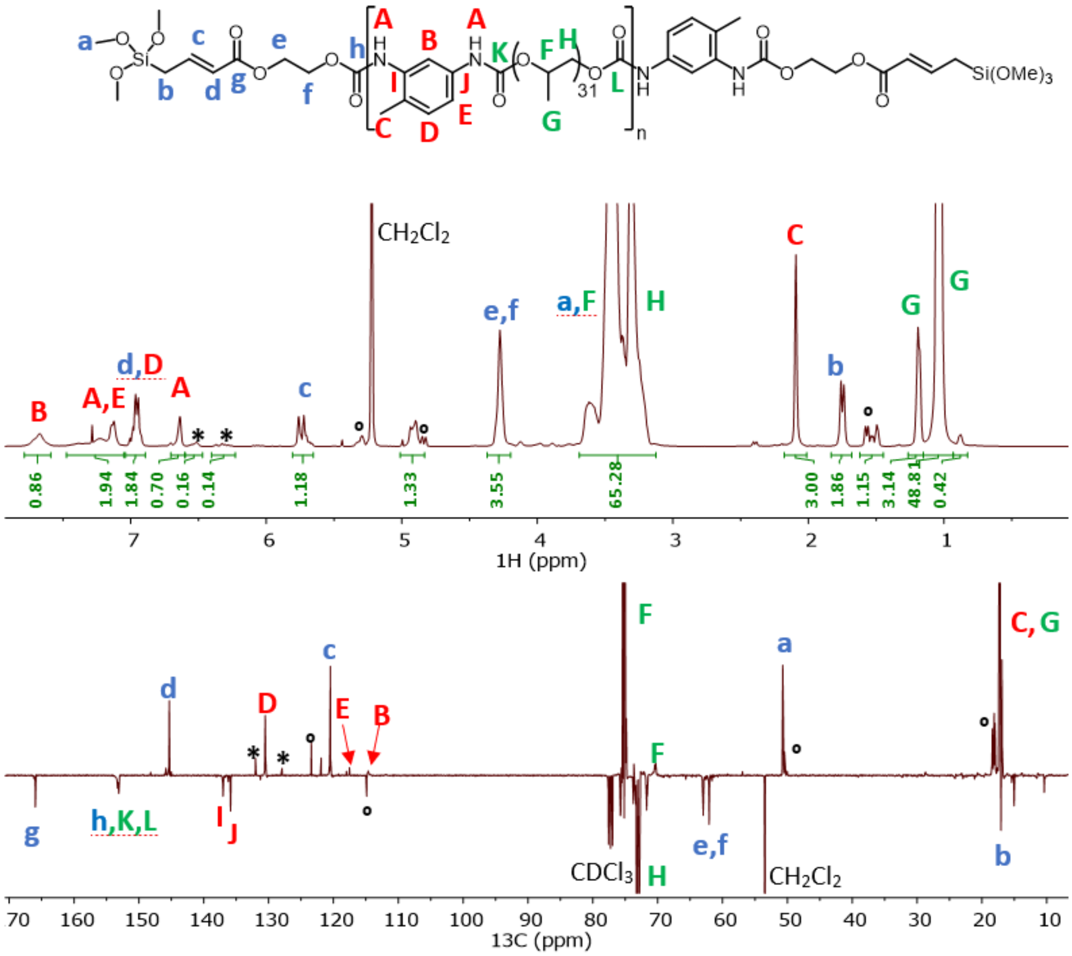

Figure S8. [1]H and J-MOD NMR spectra (400 and 100 MHz, 298 K, $CDCl_3$) of PPG*-CTA2$_2$ isolated from the CM of PPG* catalyzed by G2 using CTA2 (Table S3, entry 1); residual traces of *CTA2, and °CTA3-resulting from the self-metathesis of CTA2, not completely removed under vacuum presumably as the result of the high viscosity of the recovered polymer.

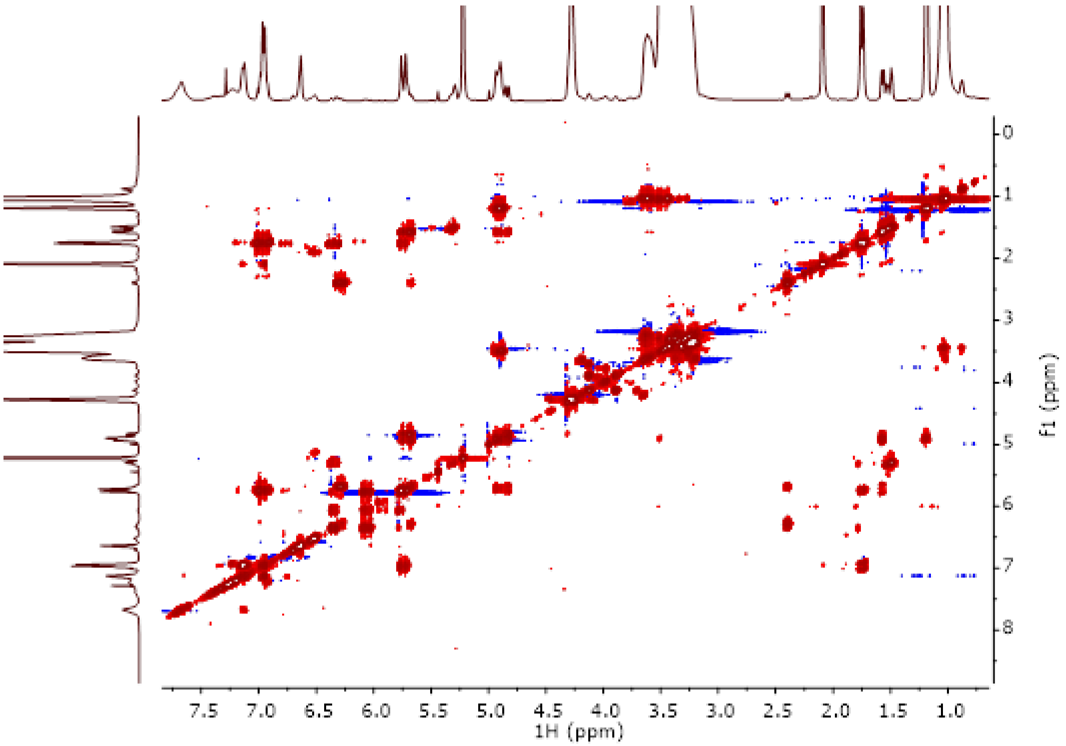

Figure S9. COSY NMR spectrum (400 MHz, $CDCl_3$, 293 K) of PPG*-CTA2$_2$ isolated from the CM of PPG* catalyzed by G2 using CTA2 (Table S3, entry 1).

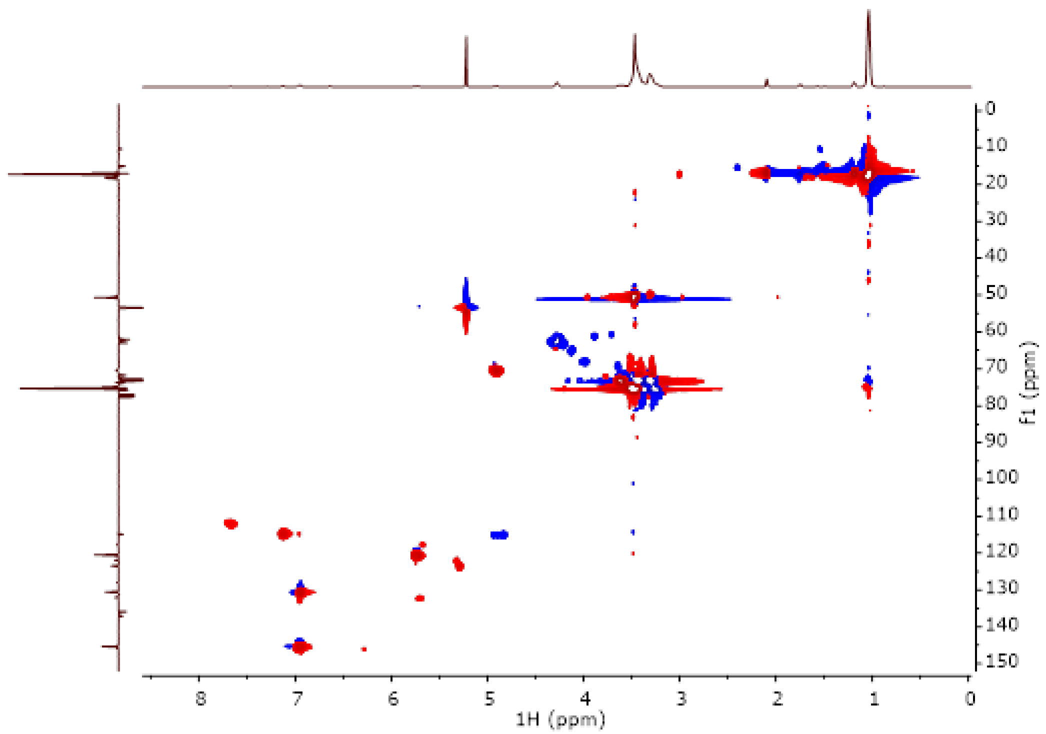

Figure S10. HSQC NMR spectrum (100 & 400 MHz, $CDCl_3$, 293 K) of PPG*-CTA2$_2$ isolated from the CM of PPG* catalyzed by G2 using CTA2 (Table S3, entry 1).

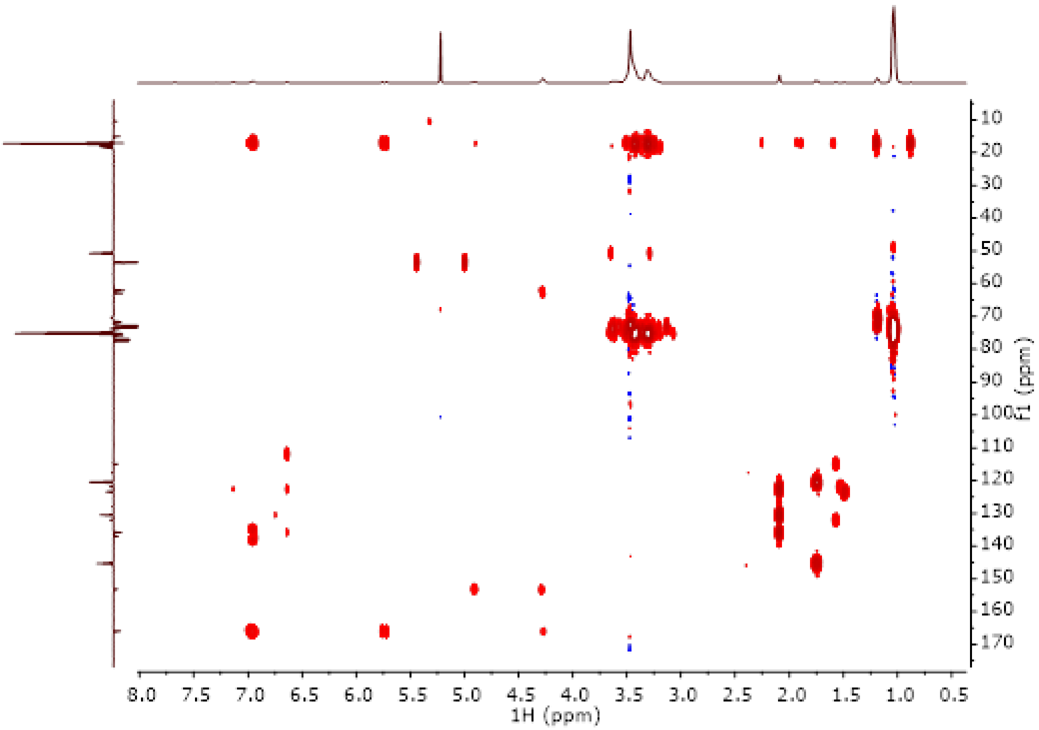

Figure S11. HMBC NMR spectrum (100 & 400 MHz, $CDCl_3$, 293 K**)** of PPG*-CTA2$_2$ isolated from the CM of PPG* catalyzed by G2 using CTA2 (Table S3, entry 1).

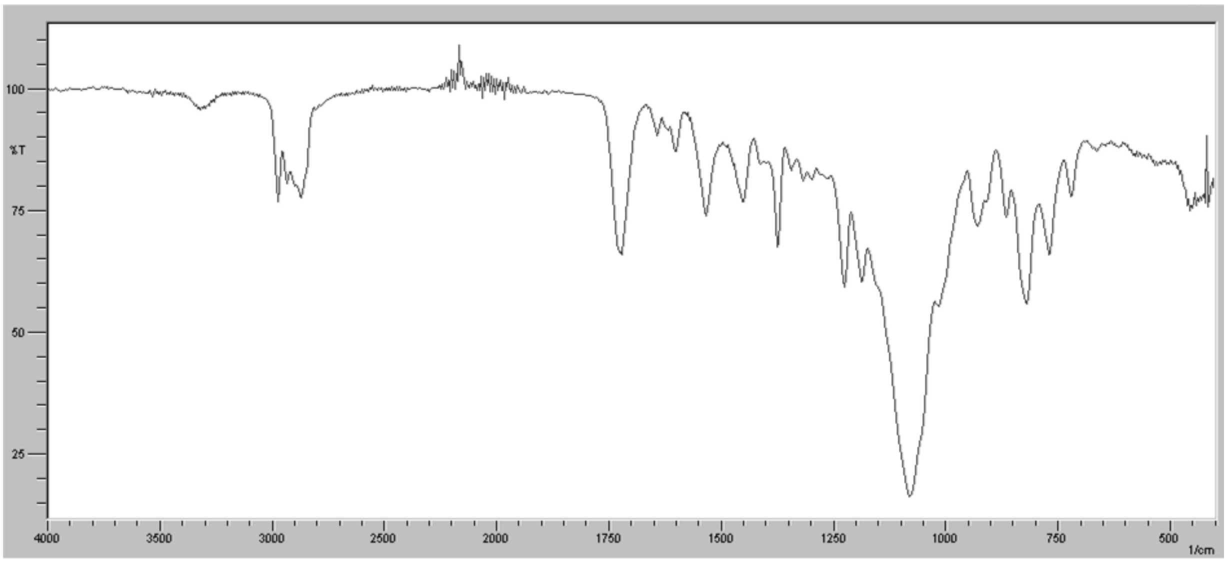

Figure S12. FT-IR spectrum of PPG*-CTA2$_2$ isolated from the CM of PPG* catalyzed by G2 using CTA2 (Table S3, entry 1).

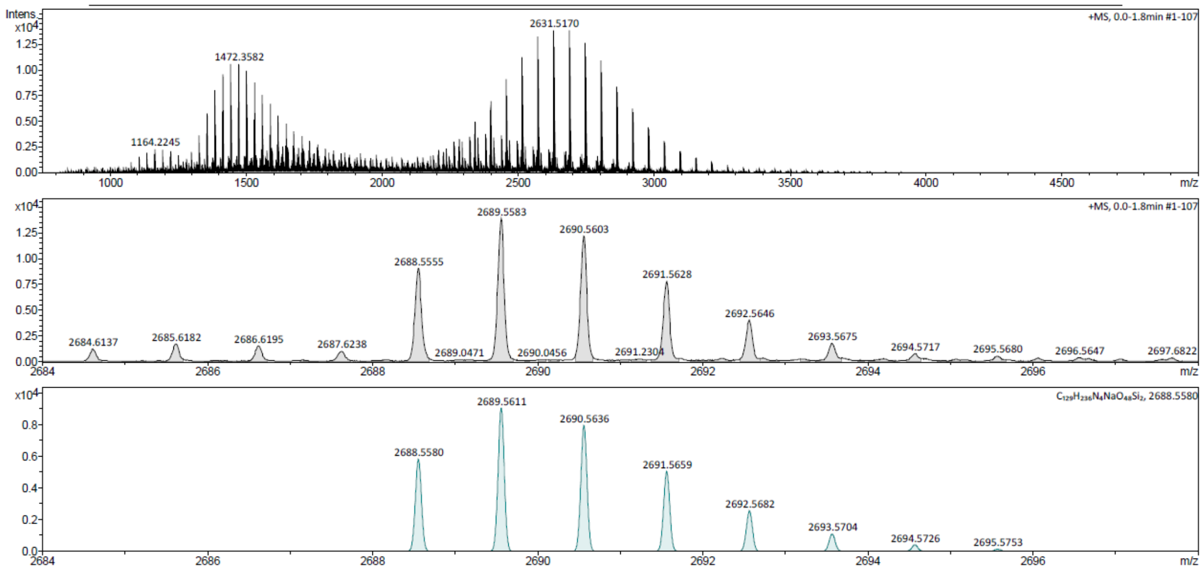

Figure S13. ESI-MS spectrum (DCTB matrix, NaI ionizing salt) of PPG*-CTA2$_2$ isolated from the CM of PPG* catalyzed by G2 using CTA2 (Table S3, entry 1); top and middle (zoomed) region: experimental spectrum, *m/z* = 900−5000 and *m/z* = 2684−2698, respectively; bottom: simulation for *m/z* = 2684−2698.

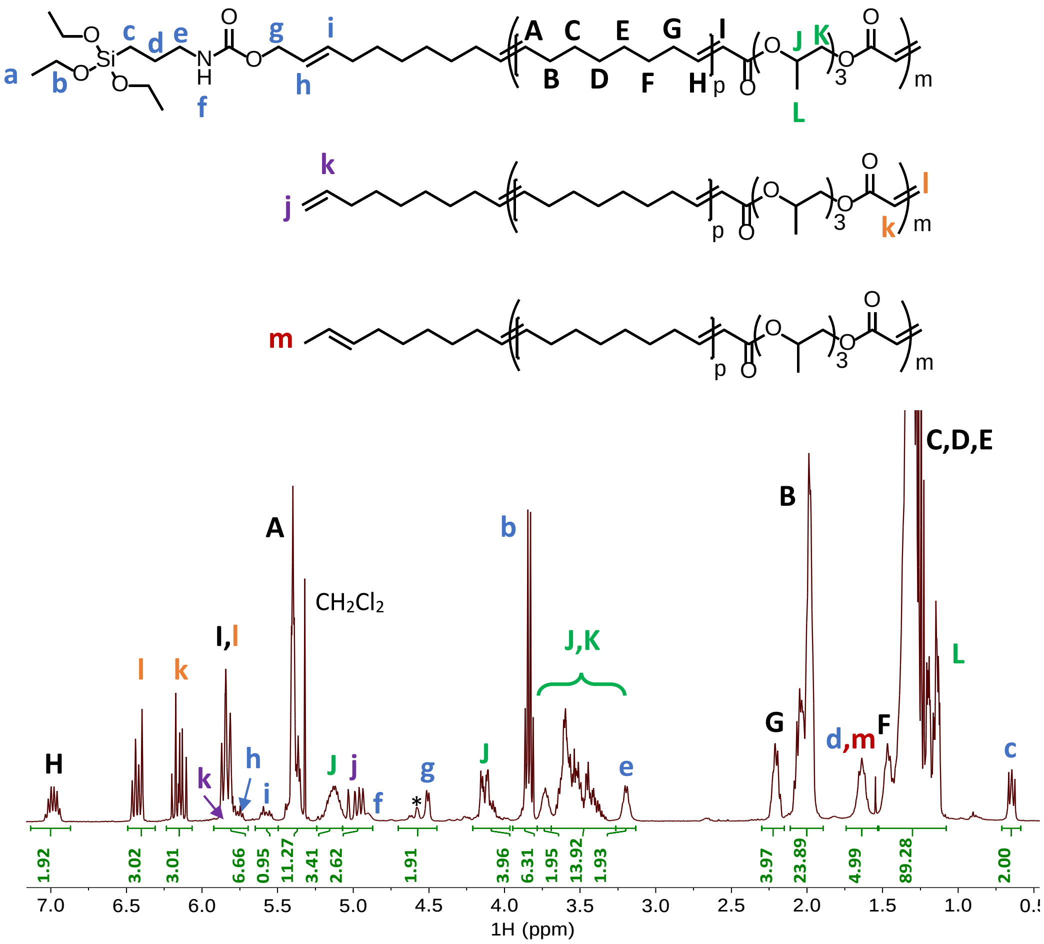

Figure S14. ^{1}H NMR spectrum (400 MHz, 23 °C, $CDCl_3$) of an α,ω-[$SiOEt_3)_2$]-PCOE/PPG crude-product prepared from the one-pot, two-step ROMP/CM-IM of COE with PPG and CTA^{Et} catalyzed by G2 (Table S6 entry 2); *: unreacted CTA^{Et}.

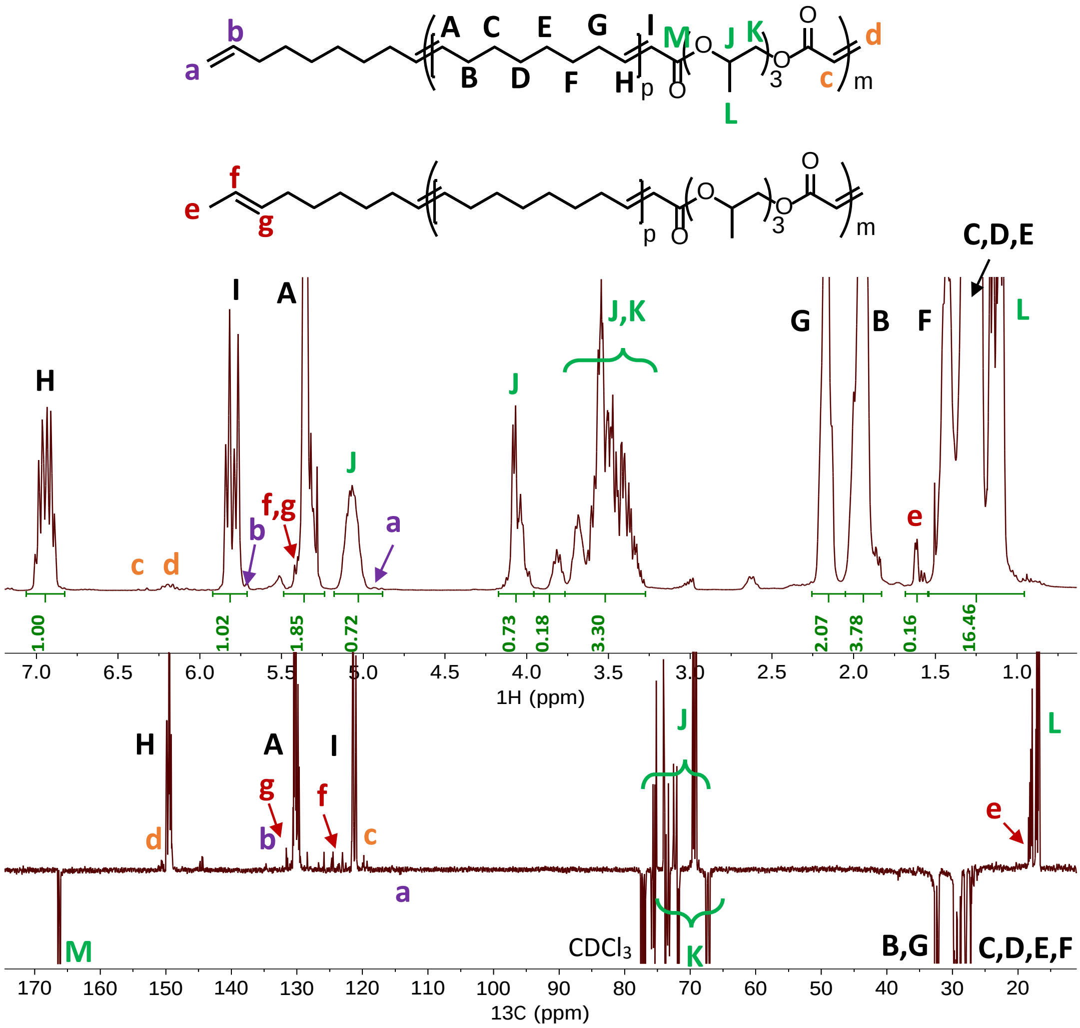

Figure S15. [1]H and J-MOD NMR spectra (400 and 100 MHz, 23 °C, $CDCl_3$) of a PCOE/PPG sample isolated from the ROIMP of COE and PPG catalyzed by G2 (Table 1, entry 2). Note that signals at δ_{1H} 2.5–3.2 ppm, 5.5 ppm; and δ_{13C} 48 ppm, 145 ppm could not be assigned.

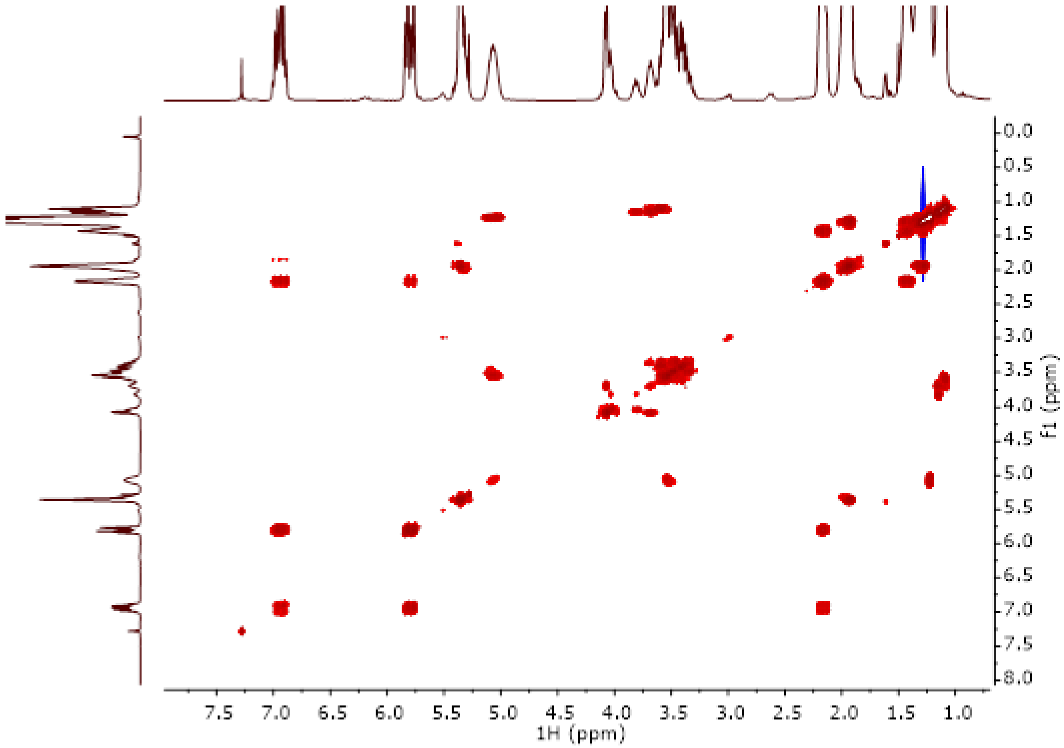

Figure S16. COSY NMR spectrum (400 MHz, 23 °C, $CDCl_3$) of a PCOE/PPG sample isolated from the ROIMP of COE and PPG catalyzed by G2 (Table 1, entry 2).

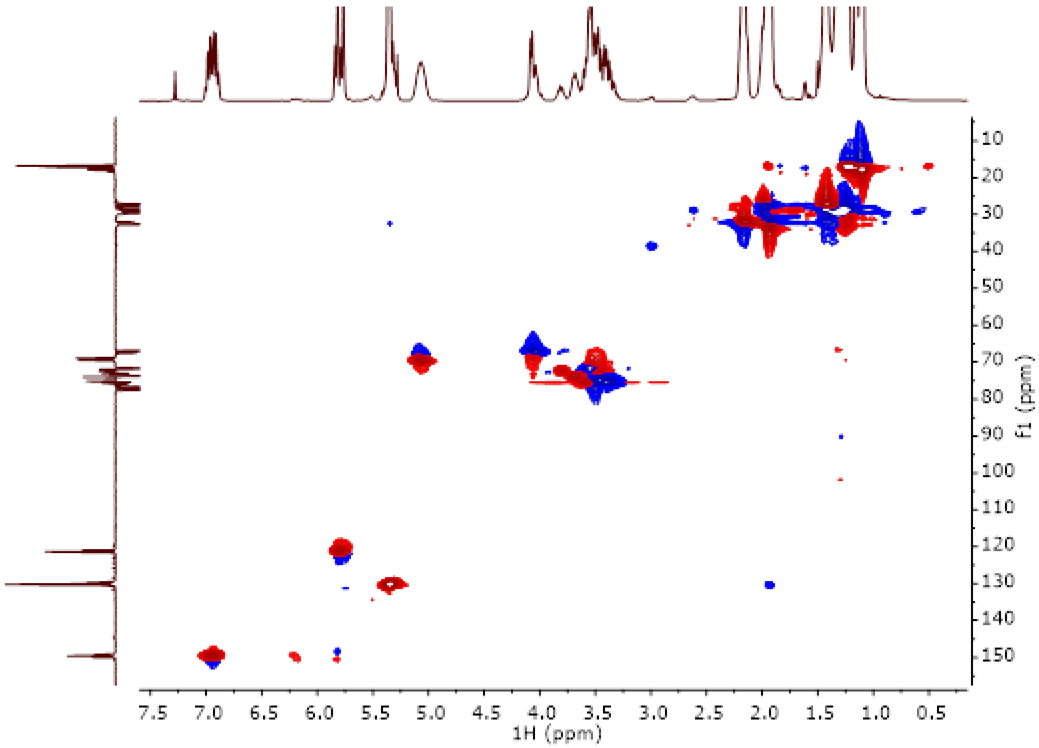

Figure S17. HSQC NMR spectrum (100 and 400 MHz, 23 °C, $CDCl_3$) of a PCOE/PPG sample isolated from the ROIMP of COE and PPG catalyzed by G2 (Table 1, entry 2).

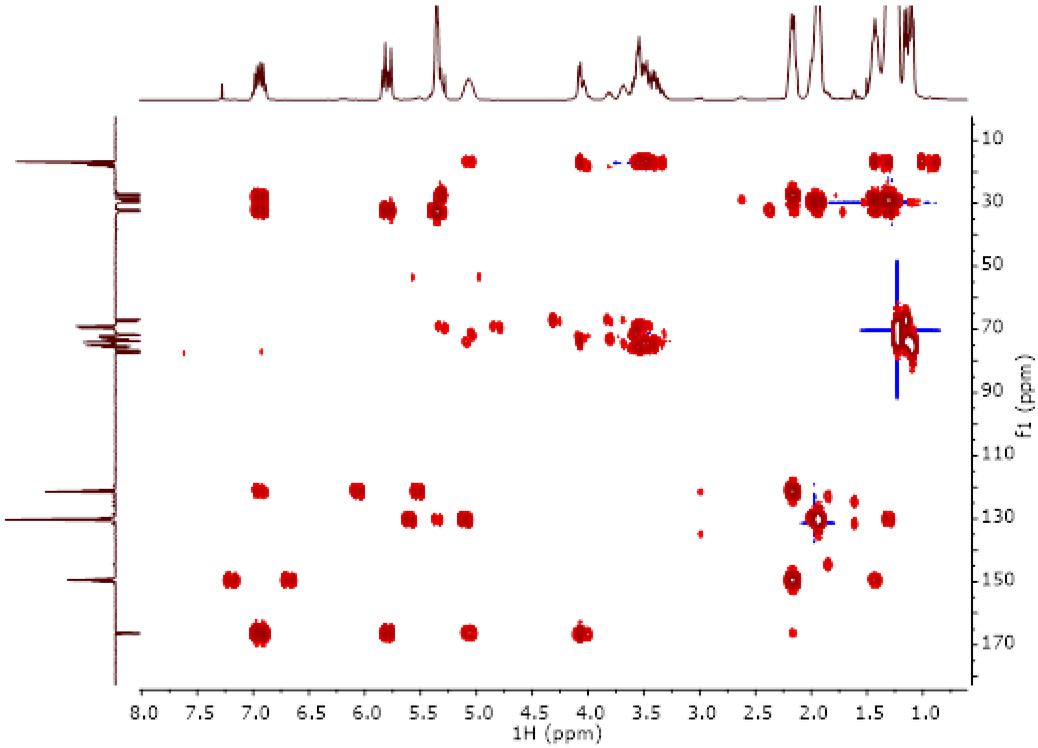

Figure S18. HMBC NMR spectrum (100 and 400 MHz, 23 °C, $CDCl_3$) of a PCOE/PPG sample isolated from the ROIMP of COE and PPG catalyzed by G2 (Table 1, entry 2).

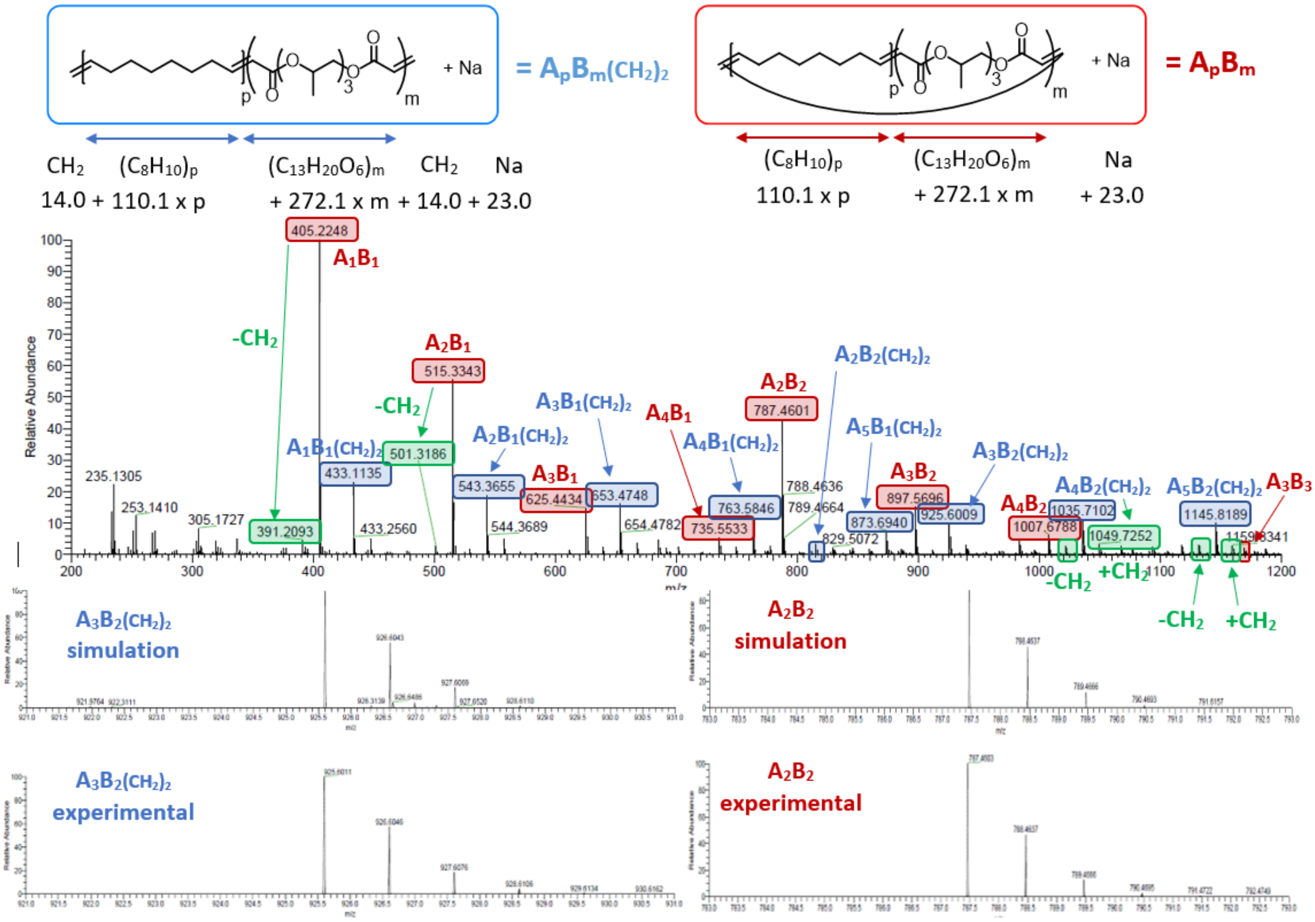

Figure S19. Top: ESI-MS mass spectrum (NaI ionizing salt) of a PCOE/PPG sample isolated from the ROIMP of COE and PPG catalyzed by G2 and recovered after removal of the solvent under vacuum (Table 1, entry 2); bottom left: simulation and experimental spectra of a linear nonfunctional (or linear isomerized) PCOE (A)/PPG (B); bottom right: simulation and experimental spectra of a cyclic PCOE (A)/PPG (B).

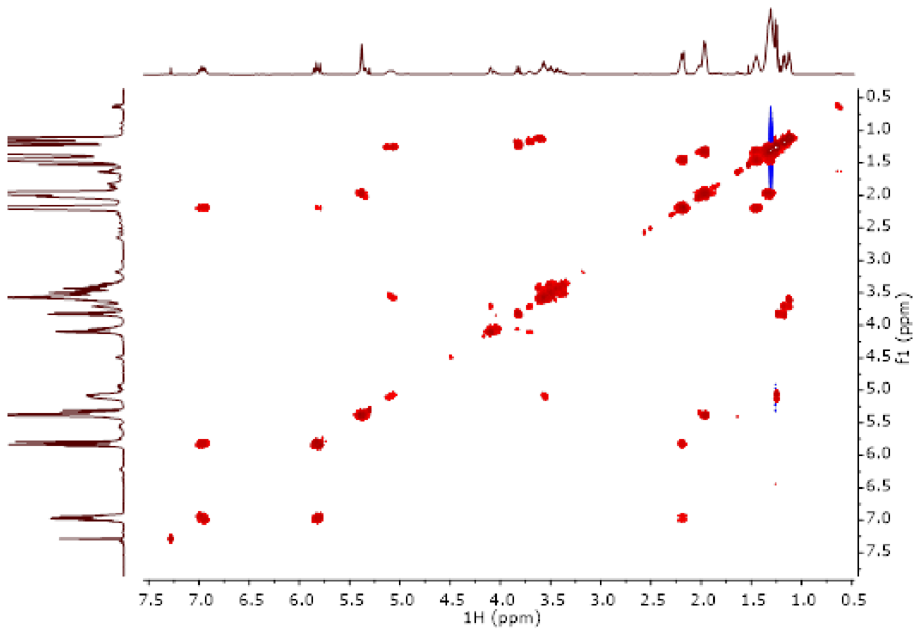

Figure S20. COSY NMR spectrum (400 MHz, 23 °C, $CDCl_3$) of an α,ω-$[Si(OEt)_3]_2$-PCOE/PPG sample isolated from the one-pot, two-step ROIMP/CM of COE and PPG catalyzed by G2 in the presence of CTA^{Et} (Table 2, entry 6).

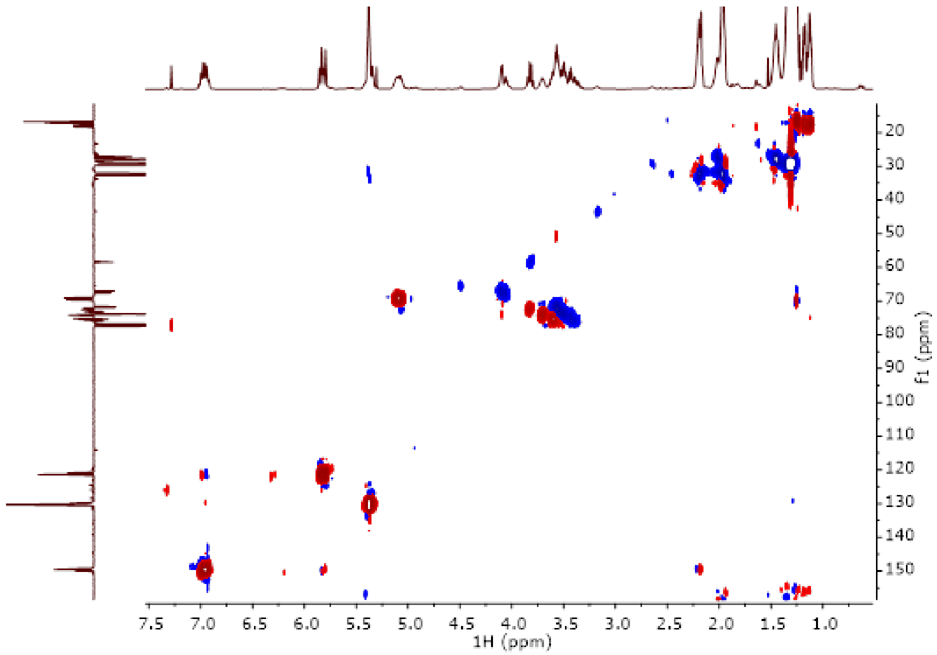

Figure S21. HSQC NMR spectrum (100 and 400 MHz, 23 °C, $CDCl_3$) of an α,ω-$[Si(OEt)_3]_2$-PCOE/PPG sample isolated from the one-pot, two-step ROIMP/CM of COE and PPG catalyzed by G2 in the presence of CTA^{Et} (Table 2, entry 6).

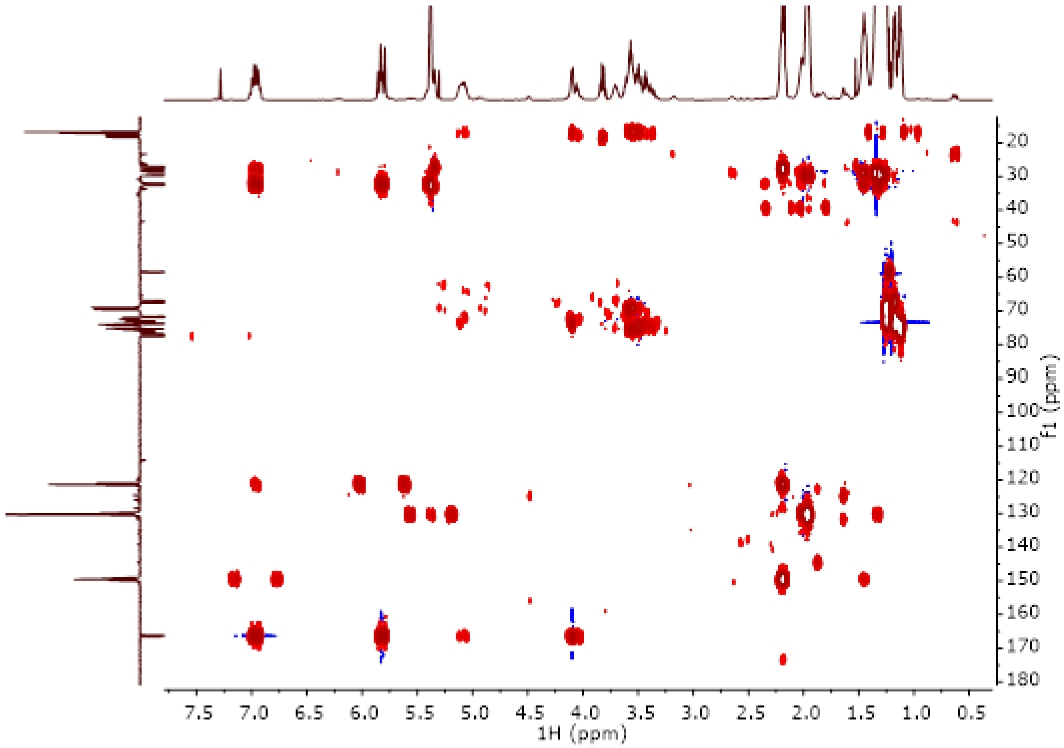

Figure S22. HMBC NMR spectrum (100 and 400 MHz, 23 °C, $CDCl_3$) of an α,ω-[$Si(OEt)_3$]$_2$-PCOE/PPG sample isolated from the one-pot, two-step ROIMP/CM of COE and PPG catalyzed by G2 in the presence of CTA^{Et} (Table 2, entry 6).

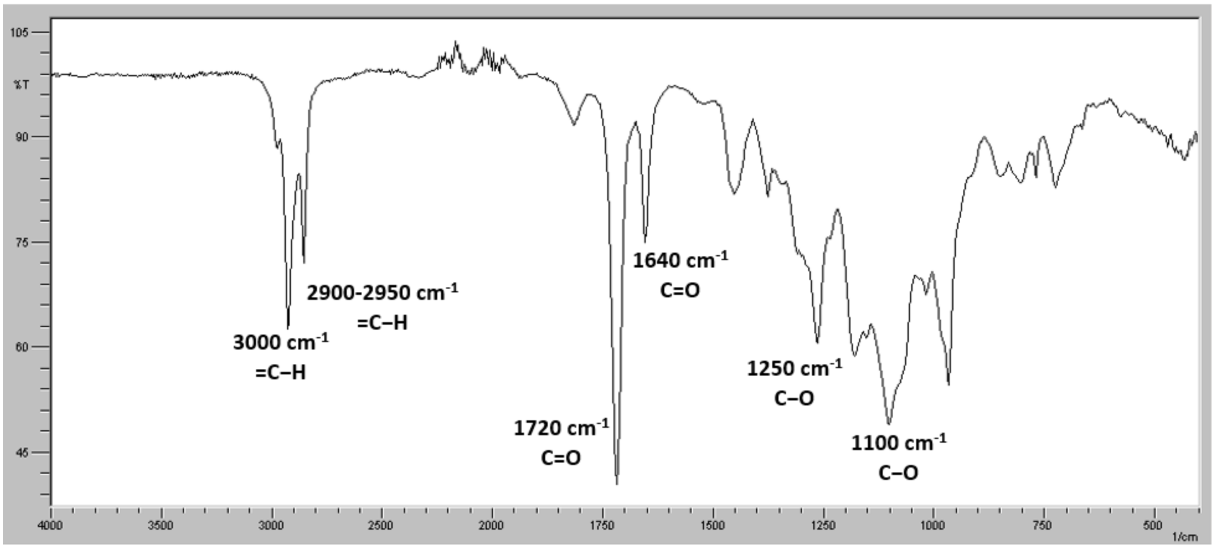

Figure S23. FT-IR spectrum of an α,ω-[$Si(OEt)_3$]$_2$-PCOE/PPG sample isolated from the one-pot, two-step ROIMP/CM of COE and PPG catalyzed by G2 in the presence of CTA^{Et} (Table 2, entry 6).

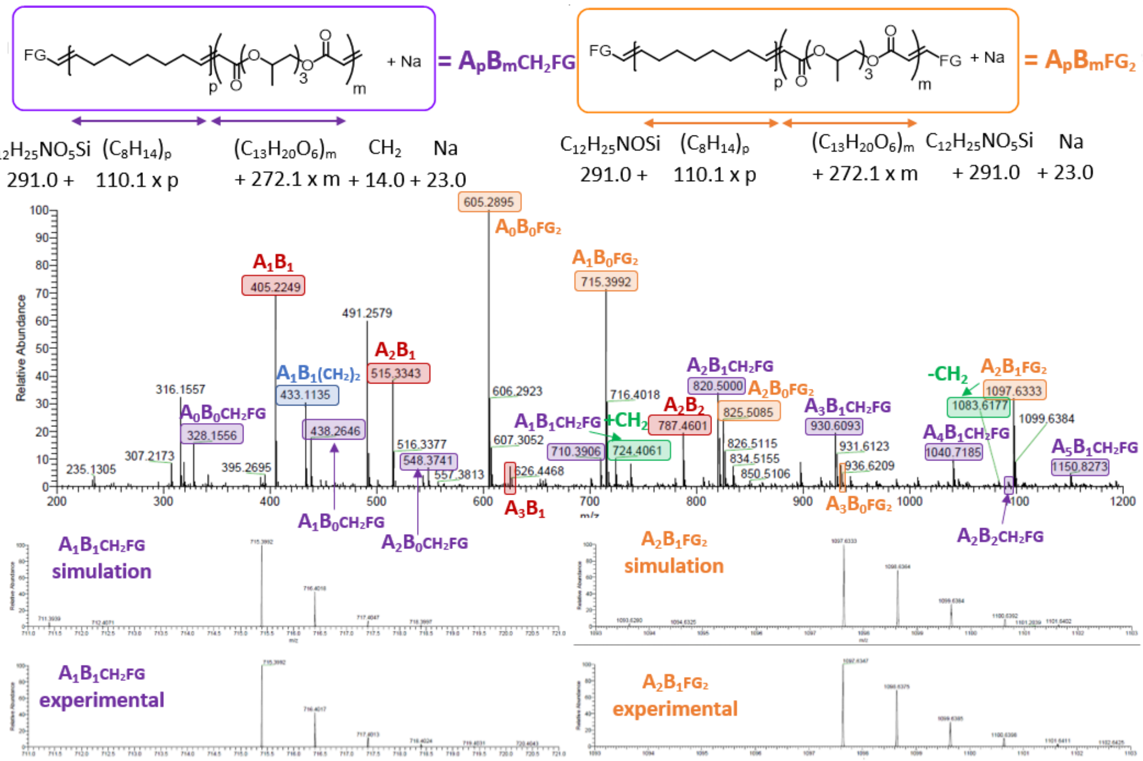

Figure S24. Top: ESI-MS mass spectrum (NaI ionizing salt; note that the Na is not made explicit in the formula of the polymer referred to as $A_pB_mCH_2FG$ and $A_pB_mFG_2$) of a α,ω-$[Si(OEt)_3]_2$-PCOE/PPG sample isolated from the one-pot, two-step ROIMP/CM of COE and PPG catalyzed by G2 in the presence of CTA^{Et} (Table 2, entry 6); bottom left: simulation and experimental spectra of a $Si(OEt)_3$-monofunctional PCOE/PPG; bottom right: simulation and experimental spectra of a $Si(OEt)_3]_2$-difunctional PCOE/PPG. For clarity, A and B refer to PCOE and PPG segments, respectively. The main population corresponds to macromolecules with a global repeating unit at m/z = 382 g.mol^{-1}, that is the sum of the molar masses of both monomers (M_{COE} + M_{PPG} = 110 + 272 g.mol^{-1}), end-capped by triethoxysilyl groups (FG = $CHCH_2OC(O)NH(CH_2)_3Si(OEt)_3$) and ionized by sodium, i.e. [FG-($PCOE_p/PPG_m$)-FG.Na^+], with e.g. m/z_{obsv} = 1097.6347 (vs. m/z_{theo} = 1097.6333) for p = 2, m = 1; in orange). In addition to this major population, some peaks were observed for nonfunctional cyclic [($PCOE_p/PPG_m$).Na^+] copolymers with m/z_{obsv} = 405.2249 (vs. m/z_{theo} = 405.2253) for p = m = 1 (population shown in red). Minor populations that correspond to (a) depletion(s) or (an) addition(s) of a CH_2 moiety in the ring opened octene chain, resulting from the internal isomerization process (Scheme S8), were identified, *e.g.* with [FG-($PCOE_p/PPG_m$)-FG.Na^+]–14 at m/z_{obsv} = 1083.6177 (vs. m/z_{theo} = 1083.6196, for m =1, p = 2), [($PCOE_p/PPG_m$)-CH_2FG.Na^+]+14 at m/z_{obsv} = 724.4061 (vs. m/z_{theo} = 724.4068, for m = p =1), [($PCOE_p/PPG_m$)-CH_2FG.Na^+] at m/z_{obsv} = 710.3906 (vs. m/z_{theo} = 710.3912, for m = p =1), and [($PCOE_p/PPG_m$).Na^+]+28 at m/z_{obsv} = 433.1135 (vs. m/z_{theo} = 433.2566, for m = p =1) (populations shown in green, green, violet and blue, respectively).

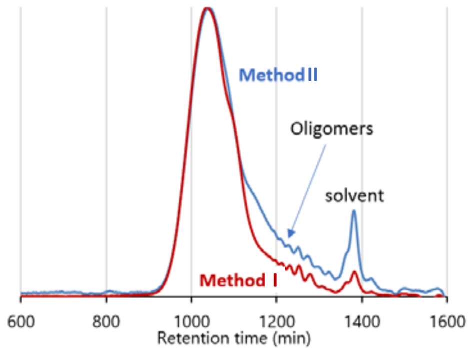

Figure S25. SEC traces (THF, 30 °C) of samples isolated from the two-step (blue – Method II) or one-step (red – Method I) ROIMP/CM of COE and PPG* catalyzed with G2 in the presence of CTA^{Et} ([COE]$_0$/[PPG*]$_0$/[CTA^{Et}]$_0$ = 1940:60:100; Table S7, entry 3, in blue and entry 4, in red).

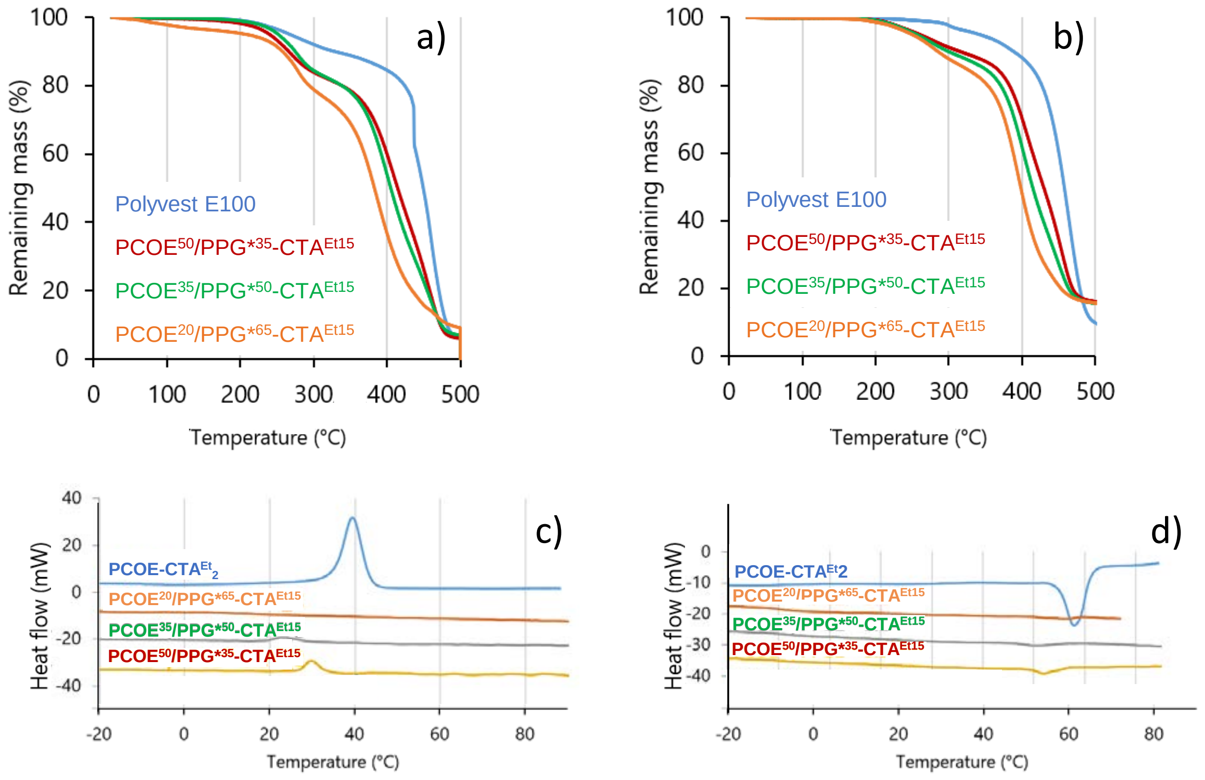

Figure S26. TGA: a) before curing; b) after curing, and DSC: c) first cooling step; d) first heating step)[6] thermograms of α,ω-$[(EtO)_3Si]_2$-PCOE/PPG* synthesized by the two-step ROIMP/CM route – large-scale synthesis Method II (Table 3).

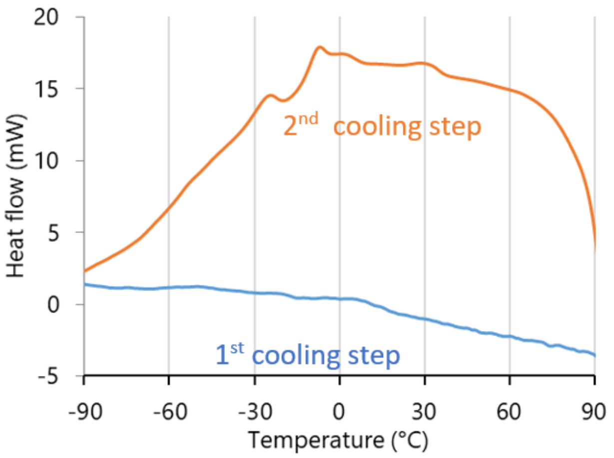

Figure S27. DSC (under helium, 10 °C.min^{-1}) thermograms of PCOE^{20}/PPG2^{65}- CTA^{Et15}, first cooling step (blue) and second cooling step (orange).

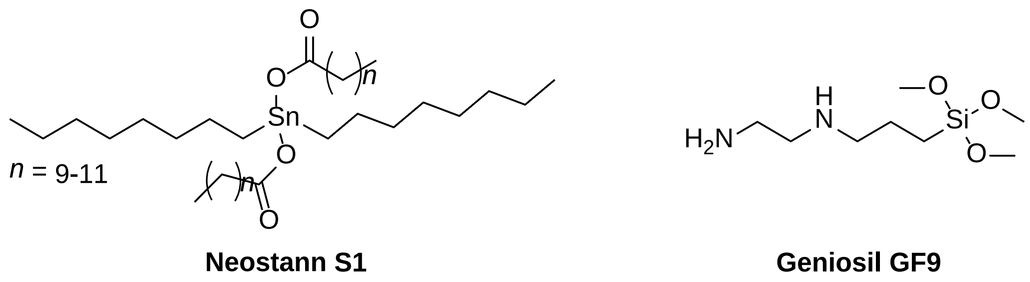

Figure S28. Structure of Neostan S1 (Kaneka) and Geniosil GF9 (Wacker).

Figure S29. Illustration of the preparation of films derived from cured α,ω-[$(EtO)_3Si]_2$-PCOE/PPG* synthesized from the two-step ROIMP/CM Method II. From left to right: mixing of the SMP and the catalytic system (S1 (1wt%) and GF9 (1wt%)); formation of the film; the film after curing (Refer to the Experiential Section).

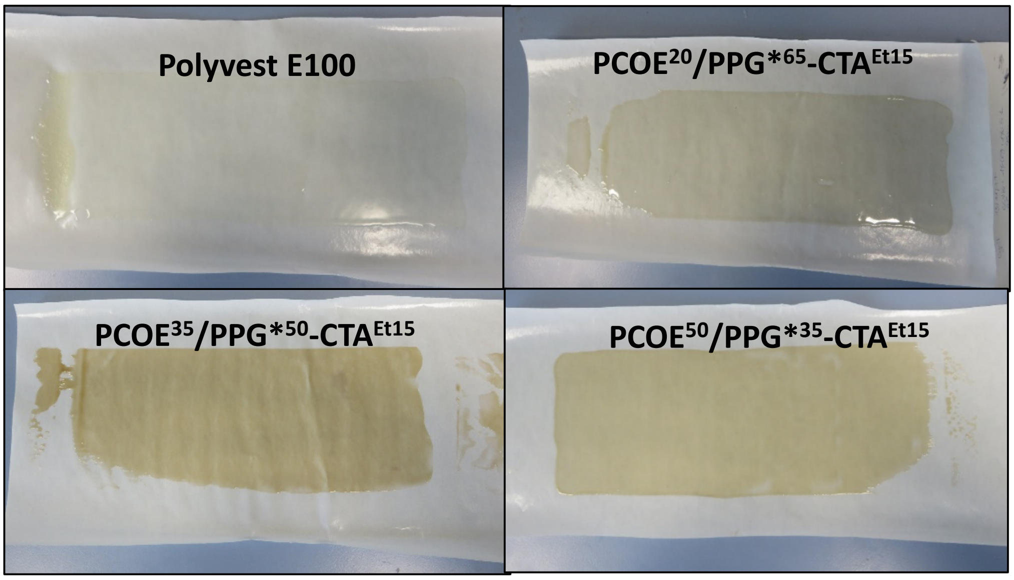

Figure S30. Examples of films obtained after curing of α,ω-$[(EtO)_3Si]_2$-PCOE/PPG* copolymers synthesized from the two-step ROIMP/CM Method II, with S1 (1wt%) and GF9 (1wt%).

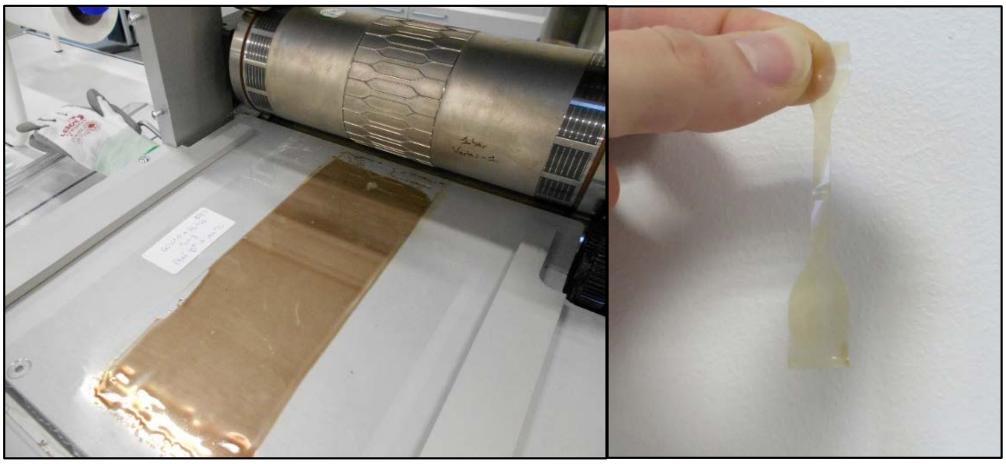

Figure S31. Left: a film obtained after curing of α,ω-$[(EtO)_3Si]_2$-PCOE/PPG* copolymers synthesized from the two-step ROIMP/CM Method II, with S1 (1wt%) and GF9 (1wt%), on the press before cutting. Right: a tensile piece cut out this film.

References

[1] Choi, T.-L.; Rutenberg, I. M.; Grubbs, R. H. Synthesis of A,B-Alternating Copolymers by Ring-Opening-Insertion-Metathesis Polymerization. *Angew. Chem. Int. Ed.* **2002**, *41*, 3839–3841.

[2] Abbas, M.; Wappel, J.; Slugovc, C. Alternating Diene Metathesis Polycondensation (ALTMET) – Opitimizing Catalyst Loading. *Macromol. Symp.* **2012**, *311*, 122–125.

[3] Michel, X.; Fouquay, S.; Michaud, G.; Simon, F.; Brusson, J.-M.; Carpentier, J.-F.; Guillaume, S. M. α,ω-Bis(Trialkoxysilyl) Difunctionalized Polycyclooctenes from Ruthenium-Catalyzed Chain-Transfer Ring-Opening Metathesis Polymerization. *Polym. Chem.* **2016**, *7*, 4810–4823.

[4] Chauveau, C.; Fouquay, S.; Michaud, G.; Simon, F.; Carpentier J.-F.; and Guillaume, S. M. α,ω-Bis(trialkoxysilyl) Telechelic Polyolefin/Polyether Copolymers for Adhesive Applications Using Ring-Opening Insertion Metathesis Polymerization Combined with a Chain-Transfer Agent. *ACS Appl. Polym. Mater.*, **2019**, *1*, 1540–1546.

[5] Note that the amount of ethylene released and of the acrylate conversion are not exactly matching. Indeed, the total amount of ethylene formed (*a priori* 100%) is divided into the ethylene released (the one we are considering) and the ethylene involved in a possible reaction with the polymer which gives non-functional chain-end groups. The amount of ethylene released has been herein determined by calculating the difference between the amount of acrylate that reacted (i.e. the amount of ethylene formed = 100%), and the sum of the amount of non-functional chain-end groups in the polymer plus the amount of isomerized chain-end groups (since no benzoquinone was used to prevent isomerization), as determined by ^{1}H NMR analyses.

[6] Due to uncontrolled polycondensation reactions observed on some SMP samples during the second cooling step (probably promoted by the high temperature and the condensation of moisture on the DSC capsule (opened, under a flux of helium) (Figure 27), only the first heating and cooling cycles were herein considered.

[7] Michel, X.; Fouquay, S.; Michaud, G.; Simon, F.; Brusson, J.-M.; Carpentier, J.-F.; Guillaume, S. M. Simple Access to Alkoxysilyl Telechelic Polyolefins from Ruthenium-Catalyzed Cross-Metathesis Depolymerization of Polydienes. *Eur. Polym. J.* **2017**, *96*, 403–413.

[8] Michel, X.; Fouquay, S.; Michaud, G.; Simon, F.; Brusson, J.-M.; Roquefort, P.; Aubry, T.; Carpentier, J.-F.; Guillaume, S. M. Tuning the Properties of α,ω-Bis(Trialkoxysilyl)

Telechelic Copolyolefins from Ruthenium-Catalyzed Chain-Transfer Ring-Opening Metathesis Polymerization (ROMP). *Polym. Chem.* **2017**, *8*, 1177–1187.

[9] Diallo, A. K.; Michel, X.; Fouquay, S.; Michaud, G.; Simon, F.; Brusson, J.-M.; Carpentier, J.-F.; Guillaume, S. M. α-Trialkoxysilyl Functionalized Polycyclooctenes Synthesized by Chain-Transfer Ring-Opening Metathesis Polymerization. *Macromolecules* **2015**, *48*, 7453–7465.

[10] Diallo, A. K.; Michel, X.; Fouquay, S.; Michaud, G.; Simon, F.; Brusson, J.-M.; Carpentier, J.-F.; Guillaume, S. M. α-Trialkoxysilyl Functionalized Polycyclooctenes Synthesized by Chain-Transfer Ring-Opening Metathesis Polymerization. *Macromolecules* **2015**, *48*, 7453–7465.